A Robust Scalable Demand-Side Management Based on Diffusion-ADMM Strategy for Smart Grid

Milad Latifi, Azam Khalili, Amir Rastegarnia, Wael M. Bazzi, and Saeid Sanei, *Senior Member, IEEE*

***Abstract*—Demand-side management (DSM) involves a group of programs, initiatives, and technologies designed to encourage consumers to modify their level and pattern of electricity usage. This is performed following methods such as financial incentives and behavioral change through education. While the objective of the DSM is to achieve a balance between energy production and demand, effective and efficient implementation of the program rests within effective use of emerging Internet of things (IoT) concept for online interactions. Here, a novel DSM framework based on diffusion and alternating direction method of multipliers (ADMM) strategies, repeated under a model predictive control (MPC) protocol, is proposed. On the demand side, the customers autonomously and by cooperation with their immediate neighbors estimate the baseline price in real time. Based on the estimated price signal, the customers schedule their energy consumption using the ADMM cost-sharing strategy to minimize their incommodity level. On the supply side, the utility company determines the price parameters based on the customers real-time behavior to make a profit and prevent the infrastructure overload. The proposed mechanism is capable of tracking drifts in the optimal solution resulting from the changes in supply/demand sides. Moreover, it considers all classes of appliances by formulating the DSM problem as a mixed-integer programming (MIP) problem. Numerical examples are provided to show the effectiveness of the proposed framework.**

***Index Terms*—ADMM, diffusion strategy, demand-side management, dual-decomposition, dynamic pricing.**

I. INTRODUCTION

In demand side management (DSM), the aggregate demand curve is flattened by effective scheduling and demand planning through smart control and rescheduling of loads, integrating renewable energies, and balancing intermittent power generation [1]. The main benefits of the DSM programs are reducing the need for new power plant, transmission and distribution networks and reducing the aggregate cost in both supply and demand sides (by efficient use of existing supply capacity), environmental improvement (by reducing greenhouse gas emissions), improving the reliability and consistency of the power system, mitigating the system urgent requirements and reducing the number of blackouts (by actively balancing the supply-demand curve).

M. Latifi, A. Khalili, A. Rastegarnia are with the Department of Electrical Engineering, Malayer University, Malayer, 65719-95863, Iran (email: milad.latifi@stu.malayeru.ac.ir; khalili@malayeru.ac.ir; rastegarnia@malayeru.ac.ir).

W. M. Bazzi is with the Electrical and Computer Engineering Department, American University in Dubai Dubai, United Arab Emirates, (email: wbazzi@aud.edu).

S. Sanei is with School of Science and Technology, Nottingham Trent University, Nottingham, NG11 8NS, UK (email: saeid.sanei@ntu.ac.uk).

Digital Object Identifier XXXXX/XXXXXXX

DSM implementation requires real-time information exchange among the electric companies, power equipments and smart meter for each user. Therefore, IoT technology has realized the possibility for implementation of DSM programs in smart grids [2]–[4]. Nevertheless, there are some challenges in using the DSM programs. The first challenge is the diversity and low flexibility of the appliance characteristics. To establish a legitimate DSM program, it is essential to consider a comprehensive and general optimization-based home energy management controller taking the exact characteristics of all the appliances into account. The next challenge to achieve an optimal DSM is to actively monitor the energy price signals coming from the utility company, participate in the energy bids, optimally respond to the energy management signals in real-time, and submit his/her scheduled energy consumption profile to the utility company by each customer. This kind of manual grid-customer interaction and granting full authority to the utility company jeopardizes the customers' privacy, reduce the utility and satisfaction level, and could result in a non-optimal management. There is, therefore, a need for developing smart systems that can autonomously execute all these tasks in a decentralized manner without prompting the customers [5]–[7].

Moreover, the integration of plug-in electric vehicles (PEVs) [8], energy storage systems (ESSs) [9], and renewable energy sources (RESs) [10] in the DSM programs plays a significant role in balancing the generation of electricity and its real-time demand. Different from the traditional computation in power systems, which customizes the information and communication technology (ICT) resources for mapping the applications separately, the DSM especially asks for scalability and economic efficiency, because there are increasing number of stakeholders participating in the computation process. Besides, handling the uncertainty resources in the system requires significant amount of calculations.

A. State of the Art

To tackle the diversity and taking the exact characteristics of all the appliances, some researches involved several classes of domestic appliances including deferrable, curtailable, thermal, and critical [11]. Others formulated multi-residential DSM problems in the smart grids with multi-class appliances models, such as [12]–[14]. An energy management method was introduced in [15] to optimally control the energy supply and the temperature settings of distributed heating and ventilation systems for residential buildings. The results showed that the

This article has been accepted for publication in a future issue of this journal, but has not been fully edited. Content may change prior to final publication. Citation information: DOI 10.1109/JIOT.2020.2968539, IEEE Internet of Things Journal

price signal fluctuations can significantly affect the DSM/DR programs. From this work we can conclude that, it is essential to consider an effective and efficient dynamic model for the price signal in such program. To benefit from the autonomous distributed methods, the customers' privacy and satisfaction level, as well as the energy provider's utility and the optimality of the distributed DSM solutions are investigated in [16]–[18].

An alternating direction method of multipliers (ADMM)-based distributed demand response (DR) method for achieving a real-time power balance in a neighborhood with a large number of customers and RESs was presented in [19] and [20], while the dynamic dc optimal power flow problem with demand response was discussed in [21]. A real-time decentralized DSM was also developed to adjust the real-time residential load to follow a pre-planned day-ahead energy generation by micro-grid [22]. A holistic formulation for energy management and trading of a Micro/Nano-grid (M/NG) with several potential components was developed in [23] to jointly optimize the internal energy consumption management and external local energy trading for a system including several M/NGs.

In recent years, the distributed autonomous DSM algorithms, such as cost-oriented cloud computing-based DSM in [24], [25], the customer-centric DSM in [26], and the computation and convergence analysis in [27] have been extensively discussed focusing on the communication/computation status of the system. In [28] a bidirectional framework for solving the demand-side management problem in a distributed way was investigated to substantially improve the search efficiency. In [29] a robust worst-case analysis was developed to tackle the uncertainties in the system. The DR problem in which the utility faces uncertainty and limited communication was discussed in [30] from utility perspective with realistic settings. A joint online learning and pricing algorithm was developed in this work to cope with the uncertainties in behavior of the price signal and customers. In [31] a pricing mechanism was implemented that relies on non-cooperative heterogeneous load knowledge of future energy consumption in the DR program with minimal amount of information. The proposed game-based DR in this work was designed in a distributed fashion converging to a Nash equilibrium with low information exchange to maintain the privacy of the customers.

B. Contributions

Considering all possible challenges, the focus here is to provide a fully distributed real-time robust DSM solution which significantly reduces the communication/computation burden on the network, secures the costumer privacy, and is autonomous in both price estimation and objective function optimization. The main contributions of this paper are as follows:

A fully distributed estimation mechanism: Because of the uncertainties (e.g., uncertainty in the generated power from the renewable resources, the customers' energy demand, and the wholesale electricity price) applying the DSM and DR strategies in a day-ahead manner is not accurate and therefore real-time mechanisms are necessary. In one hand, to make an optimal decision in a real-time application, the customers need to know the electricity price in the upcoming time-slots. On the other hand, the exact electricity price is revealed at the end of each slot, after the power is consumed and the utility company becomes aware of its value. So, there is a need for an agent-based (to maintain the privacy of the customers), adaptive real-time (to act on time), and fully distributed (to be practical) mechanism by which the customers can estimate the electricity price variation accurately. The estimation mechanism must be robust to communication disruptions to increase the reliability of the power system. None of the presented works in the literature has investigated such issues. For the first time, an autonomous fully distributed price estimation mechanism using a powerful, robust, and scalable adaptive diffusion-least mean square (LMS) strategy is developed as the first contribution of this paper. By applying the proposed strategy, the customers can cooperatively estimate the price signal for the upcoming scheduling window and update it adaptively at each time slot using the already received information.

A novel cost-sharing optimization mechanism: After the price estimation, the customers must consider the impact of their decisions on the price function and subsequently have a better intuition on the electricity price in the upcoming time slots. Enabling such capability in a distributed manner needs the customers to know the power consumption of each other [32]–[34]. However, the consumption pattern of each customer is its private information. Further, performing the DSM algorithm by the customers sequentially (as done by the game theoretic methods) imposes a long delay to the system which is not acceptable in real-time applications. The second contribution of this paper is to tackle the above two issues by formulating a novel supply-bidding function and applying the ADMM mechanism to the DSM program. Despite the present ADMM approaches, such as [19]–[21] which only take part in the optimization problem, the proposed ADMM optimization mechanism in this paper is synchronized with the supply-bidding functions and price estimation mechanism due to its cost-sharing protocol. By the formulated synchronized cost-sharing ADMM method, the estimation and optimization part of the DSM framework is implemented simultaneously, the privacy of the customers are preserved (as each customer only needs to know the average power consumption of the system) and they can run their DSM algorithms simultaneously which lowers the time delay.

A computationally efficient optimization algorithm: By increasing the number of customers and the power grid scale, there is an essential need for a simple optimization method with low computational cost of real-time implementation. However, the characteristic of some electrical appliances may lead to generation of integer variables, which in turn, change the DSM problem as a mixed-integer programming (MIP) problem and increase the complexity of the optimization problem. Given some existing solutions to an MIP, the third contribution of this paper is to provide a simple but effective solution to this problem by converting the integer variables into continuous variables and providing an augmentation-based penalty (AbP) to guarantee an acceptable accuracy in approximating the integer variables. ***A dynamic pricing***

This article has been accepted for publication in a future issue of this journal, but has not been fully edited. Content may change prior to final publication. Citation information: DOI 10.1109/JIOT.2020.2968539, IEEE Internet of Things Journal

TABLE I
SUMMARY OF NOTATION.

Symbol	Description	Symbol	Description
$\mathcal{K}, K, k$	Set of customers, total number of customers, and their index	$E^{cap}_{k,b}$	The capacity of storage device b of customer k
$\mathcal{H}, H, h$	Set of equal length time slots, scheduling horizon, and time slot index	$\eta^c_{k,b}$	Charging efficiency of storage device b of customer k
$\mathcal{A}_k, A_k, a, b$	Set of customer k's appliances, total number of these appliances, and appliance indexes	$\eta^d_{k,b}$	Discharging efficiency of storage device b of customer k
$\mathcal{A}^{no}_k$	Set of customer k's non-flexible appliances	l^h_k	Total energy demand of customer k at time slot h
$\mathcal{A}^{lf}_k$	Set of customer k's low-flexible appliances	$l^{\min}$	The capacity of the power system's infrastructure (reverse current)
$\mathcal{A}^{mf}_k$	Set of customer k's mid-flexible appliances	$l^{\max}$	The capacity of the power system's infrastructure (direct current)
$\mathcal{A}^{hf}_k$	Set of customer k's high-flexible appliances	$\mathbf{X}_k$	customer k's consumption profile throughout the scheduling horizon H
$\mathcal{H}_{k,a}$	Set of permissible time slots for scheduling operation of appliance a of customer k	$p^h, \tilde{p}^h_{bl}, p^h_{sh}$	Price signal determined for time slot h, the baseline part, the shadow part
$\alpha_{k,a}$	Minimum start time of operation for appliance a of customer k	$U^h_{k,a}(\cdot)$	Concave utility function of appliance a if customer k
$\beta_{k,a}$	Maximum end time of operation for appliance a of customer k	$w^h_{k,a}$	Priority of energy consumption index at slot h related to appliance a of customer k
$E^{min}_{k,a}$	Minimum tolerable energy demand bounds of appliance $a \in \mathcal{A}^{hf}_k$ of customer k	$r^u_{k,a}$	Upper bound of the corresponding integer variable $x^{h,in}_{k,a}$
$E^{max}_{k,a}$	Maximum tolerable energy demand bounds of appliance $a \in \mathcal{A}^{hf}_k$ of customer k	λ_k	Weight factor for making trade-off between minimizing cost and maximizing utility
$E_{k,a}$	Total desirable energy need of appliance $a \in \mathcal{A}^{hf}_k$ of customer k for finishing its task	μ^h_u, μ^h_d	Lagrange multipliers at slot h
$x^{min}_{k,a}$	Minimum power level that appliance $a \in \mathcal{A}^{hf}_k$ of customer k can consume	$G_{k,g}(\mathbf{X}^{in}_k), g_k$	Set of affine constraints induced by integer variables $\mathbf{X}^{in}_k$ and total number of these constraints for customer k
$x^{max}_{k,a}$	Maximum power level that appliance $a \in \mathcal{A}^{hf}_k$ of customer k can consume	$\delta^{EP}(x)$	Penalty function for affine constraints with parameter η_k
$x^h_{k,a}$	Power consumption rate scheduled for appliance a of customer k at time slot h	$\tilde{v}^h_k$	zero-mean random price estimation noise
$\Gamma^h_{k,a}$	Auxiliary variable, equal to 1 if appliance a of customer k turned on at slot h, while was off at slot $h-1$, otherwise is equal to 0.	$\tilde{z}^h_k$	Vector of the explanatory data available at customer k at slot h
$x^{rat}_{k,a}$	The nominal power consumption by appliance a of customer k	μ_k, ν_k	Step sizes for adaptation and combination phases
$E^{fix}_{k,a}$	Total desirable energy need of appliance a of customer k for finishing its task	$\mathcal{N}_k$	Set of neighborhood of customer k
$E^h_{k,b}$	The energy level of storage device b of customer k at slot h	$a_{l,k}, c_{l,k}$	Weight parameter for adaptation and combination phases

policy: The system supply capacity and the aggregate load demand fluctuations are other highly important issues which are not modeled and considered explicitly in the mentioned works. From the presented simulation results, increasing the involvement of DSM programs to the power system can put the reliability and stability of the power systems into danger. This is because all the customers try to consume more power in the low-price slots and sell it in the high-price slots (i.e., the high revers-current). This can create sub-peaks and high load fluctuations. In the mentioned works (such as, [9], [10], [15], [30], [31]) these peak loads and high demand fluctuations can overload all the distribution infrastructures and take down the power system. To prevent such damages and provide a valid DSM approach we provide a dynamic pricing policy. The role of this policy is to impose a high shadow-price to the customers whose consumption patterns tend to deviate from the aggregate optimal power flow and violate the supply capacity limit. Specifically, when all the customers try to consume more power in the low baseline-price time-slots, which has a potential to over cross the system supply capacity, the shadow-price increases to reduce the customers' incentive in consumption in those time-slots. To manage this, we need to couple the amount of total customers' power consumption to each other through imposing a sharing cost function and a constraint on the aggregate allowed maximum/minimum power flow of the system infrastructure. On the other hand, to be able to still implement a fully distributed DSM mechanism, a dual-decomposition technique is proposed to uncouple the customers decisions, while guaranteeing that the total demand does not exceed the power infrastructure capacity. This is the last contribution of the paper.

The rest of this paper is organized as follows. In Section II, we present the considered smart grid model. The DSM problem is formulated in Section III. In Section IV we explain the proposed Diffusion-ADMM strategy model in detail. Section V shows the simulation results and we conclude the paper in Section VI.

Notation: Throughout the paper, the scalars are denoted by normal fonts, sets are denoted in calligraphy mode, and vectors by boldface lower-case and matrices by boldface upper-case letters. We show the expectation operator by $\mathbb{E}[\cdot]$, the matrix transpose by $(\cdot)^\top$, and the conjugate by $(\cdot)^*$. $\tilde{x}$ implies that x is stochastic and we denote its estimate by $\hat{x}$. $\mathbb{1}$ denotes a column vector with unit entries and $\mathtt{tr}(\cdot)$ denotes the trace operator. The other notations are listed in Table I.

II. SYSTEM MODEL

Consider an architecture consisting of one energy provider (i.e., the utility company) and a set of $\mathcal{K} = \{1, 2, \cdots, K\}$

This article has been accepted for publication in a future issue of this journal, but has not been fully edited. Content may change prior to final publication. Citation information: DOI 10.1109/JIOT.2020.2968539, IEEE Internet of Things Journal

residential customers (with the total number $K \triangleq |\mathcal{K}|$). As is common in the DSM literature, we assume that each customer is equipped with a smart meter (SM) including an energy consumption manager (ECM) device with the ability of energy consumption scheduling of its appliances. All the customers' smart meters are connected to the same utility company and their neighbors through a suitable two-way communication protocol, i.e., a local area network (LAN). The utility company is, in turn, connected to the wholesale market to provide its customers' demand. The set of equal length time slots (h) in the scheduling horizon is $\mathcal{H} = \{1, 2, \cdots, H\}$. Further, $\mathcal{A}_k$ and $A_k \triangleq |\mathcal{A}_k|$ denote the set of all appliances and the total number of appliances belonging to customer k, respectively.

Each customer is assumed to have probably a storage device and four classes of appliances with non-flexible (e.g., refrigerator), high-flexible (e.g., PEV), mid-flexible (e.g., pool pump), and low-flexible (e.g., washing machine) characteristics denoted as $\mathcal{A}_k^{no}$, $\mathcal{A}_k^{hf}$, $\mathcal{A}_k^{mf}$, and $\mathcal{A}_k^{lf}$, respectively. Each appliance $a \in \mathcal{A}_k = \mathcal{A}_k^{no} \times \mathcal{A}_k^{hf} \times \mathcal{A}_k^{mf} \times \mathcal{A}_k^{lf}$ has its own allowed scheduling window $\mathcal{H}_{k,a} \triangleq \{\alpha_{k,a}, \cdots, \beta_{k,a}\}$, where $\alpha_{k,a}$ is the minimum possible start time and $\beta_{k,a}$ is the maximum acceptable end time of the operation. We define the specifications of these appliances as follows:

$$
\begin{aligned}
& x_{k,a}^{min} \le x_{k,a}^h \le x_{k,a}^{max}, \ \forall a \in \mathcal{A}_k^{hf} \text{ and } h \in \mathcal{H}, \\
& E_{k,a}^{min} \le E_{k,a} \le E_{k,a}^{max}, \ \sum_{h=\alpha_{k,a}}^{\beta_{k,a}} x_{k,a}^h = E_{k,a}, \ \forall a \in \mathcal{A}_k^{hf}, \\
& x_{k,a}^h \in \{0, x_{k,a}^{rat}\}, \ \Gamma_{k,a}^h \in \{0,1\}, \ \forall a \in \mathcal{A}_k^{mf} \times \mathcal{A}_k^{lf} \text{ and } h \in \mathcal{H}, \\
& \sum_{h=\alpha_{k,a}}^{\beta_{k,a}} \Gamma_{k,a}^h x_{k,a}^h = E_{k,a}^{fix}, \ \sum_{h=\alpha_{k,a}}^{\beta_{k,a}} \Gamma_{k,a}^h \ge 1 \ \forall a \in \mathcal{A}_k^{mf}, \\
& \sum_{h=\alpha_{k,a}}^{\beta_{k,a}} \Gamma_{k,a}^h \sum_{i=h}^{h+\Delta_{k,a}-1} x_{k,a}^i = E_{k,a}^{fix}, \ \sum_{h=\alpha_{k,a}}^{\beta_{k,a}-\Delta_{k,a}+1} \Gamma_{k,a}^h = 1, \ \forall a \in \mathcal{A}_k^{lf}
\end{aligned}
\tag{1}
$$

where $x_{k,a}^h$ ($= 0, \ \forall \ h \notin \mathcal{H}_{k,a}$) is the power consumption rate scheduled by the ECM of customer k for his appliance a at time slot h with minimum and maximum power rate bounds $x_{k,a}^{min}$ and $x_{k,a}^{max}$. The first and second lines of (1) refer to the high-flexible appliances, where $E_{k,a}$ is the desired aggregated energy which must be consumed until $\beta_{k,a}$, with the minimum and maximum tolerable energy bounds $E_{k,a}^{min}$ and $E_{k,a}^{max}$. Third line of (1) belongs to the mid-flexible and low-flexible appliances expressing that these appliances work with their nominal power $x_{k,a}^{rat}$ regulated by an auxiliary variable $\Gamma_{k,a}^h = \{0 \text{ (off mode)}, 1 \text{ (on mode)}\}$. The forth line implies that the mid-flexible appliances need fixed amount of energy $E_{k,a}^{fix}$ until $\beta_{k,a}$, while the operation of them can be interrupted and resume again. The last line expresses that once the low-flexible appliances switch on, their operations cannot be interrupted until the end of their tasks. That means, $\Gamma_{k,a}^h$ works as a trigger for the low-flexible appliance and once is equal to one, the appliance continue working for a continuous period with length $\Delta_{k,a} = E_{k,a}^{fix}/x_{k,a}^{rat}$. This operation period is the time needed for the low-flexible appliance to finish its work while continuously works with the nominal power rate $x_{k,a}^{rat}$. As the appliance's task must be finished before the deadline $\beta_{k,a}$, the second constraint of the last line implies that the appliance must be turned on before $h = \beta_{k,a} - \Delta_{k,a}$.

The customer can procure energy to his appliances from either the utility company or by providing from his own storage device. However, the storage device energy level and charge/discharge power rates are limited at each slot h as:

$$
0 \le E_{k,b}^h \le E_{k,b}^{cap}, \ -x_{k,b}^{rat} \le \Gamma_{k,b}^h x_{k,b}^h \le x_{k,b}^{rat}, \ \forall h \in \mathcal{H} \tag{2}
$$

where $E_{k,b}^h = E_{k,b}^{h-1} + x_{k,b}^h\big[(\Gamma_{k,b}^h + 1)\eta_{k,b}^c + (\Gamma_{k,b}^h - 1)/\eta_{k,b}^d)\big]/2$ is the energy level of storage device of customer k updated at slot h, with the charring/discharging efficiencies denoted respectively as $0 < \eta_{k,b}^c < 1$ and $0 < \eta_{k,b}^d < 1$. Using auxiliary variable $\Gamma_{k,b}^h = \{-1 \text{ (discharge mode)}, 0 \text{ (idle mode)}, 1 \text{ (charge mode)}\}$ the dynamic evolution of energy level of the battery is updated. Namely, when $\Gamma_{k,b}^h = 1$ at slot h, the charge rate $\Gamma_{k,b}^h x_{k,b}^h > 0$ is the amount of power consumed by the battery, while the fraction $\eta_{k,b}^c x_{k,b}^h$ of it added to $E_{k,b}^{h-1}$ and stored in the battery. As the same way, when $\Gamma_{k,b}^h = -1$ at slot h, the discharge rate $\Gamma_{k,b}^h x_{k,b}^h < 0$ is the amount of power delivered by the battery, while the power amount $x_{k,b}^h/\eta_{k,b}^d$ is actually drawn from the battery and is subtracted from $E_{k,b}^{h-1}$. Without loss of generality by ignoring the battery self-discharge rate, we have $E_{k,b}^h = E_{k,b}^{h-1}$ when the battery is in idle mode (i.e., $x_{k,b}^h = 0$).

There is usually a constraint on the total permissible energy consumption over the power grid at each time slot h:

$$
l^{min} \le \sum_{k \in \mathcal{K}} l_k^h \le l^{max}, \quad \forall \ h \in \mathcal{H} \tag{3}
$$

where $l_k^h = \sum_{a \in \mathcal{A}_k} x_{k,a}^h$ and l^{max} is the maximum aggregate amount of energy that the customers can demand from the utility company at each time slot. If the utility company has ability to sell electricity back to the main grid, we can let $l^{min} < 0$, otherwise $l^{min} = 0$. In fact, this constraint prevents creation of sub-peaks at the low-price time slots, or exceeding the demand from the capacity of system's infrastructure (overloading).

III. Problem Formulation

The social welfare problem may be given as:

$$
\max_{\boldsymbol{X} \in \mathcal{X}} \sum_{h \in \mathcal{H}} \Big(\sum_{k \in \mathcal{K}} \sum_{a \in \mathcal{A}_k} U_{k,a}^h(x_{k,a}^h, w_{k,a}^h) - C^h(\sum_{k \in \mathcal{K}} \sum_{a \in \mathcal{A}_k} x_{k,a}^h) \Big) \tag{4}
$$

where $\mathcal{X}$ is the global feasible set constructed of constraints (1), (2), and (3) for all the customers, and $U_{k,a}^h(\cdot)$ is a concave utility function[1] representing the satisfaction level of appliance a belonging to customer k with priority factor $w_{k,a}^h$ for slot h. The total cost imposed on the utility company for supplying (generation/transmission/distribution) power at slot h, $C^h(x) = \vartheta_1 x^2 + \vartheta_2 x + \vartheta_3$, is strictly convex, where ϑ_1, ϑ_2, and ϑ_3 are some appropriate parameters.

Remark 1. The proposed appliance model/constraints set in $\mathcal{X}$ is quite general and can be adopted for any appliance

[1] In general, a utility function describes the level of *usefulness* of available resources and the quality of energy used by the customers.

This article has been accepted for publication in a future issue of this journal, but has not been fully edited. Content may change prior to final publication. Citation information: DOI 10.1109/JIOT.2020.2968539, IEEE Internet of Things Journal

by changing some model parameters. For example, a well-known nonlinear switching model for thermostatically controlled loads (TCLs) is as follows [35]:

$$\theta_{k,c}^{h} = M_1 \theta_{k,c}^{h-1} + (1 - M_1)(\theta_A - M_2 \Gamma_{k,c}^{h} x_{k,c}^{rat}) \quad (5)$$

where $\theta_{k,c}^{h}$ is the temperature of TCL c of customer k at time-slot h, θ_A is the ambient temperature whose dynamics are much slower than $\theta_{k,c}^{h}$, $x_{k,c}^{rat}$ is the rated power, and $\Gamma_{k,c}^{h} \in \{0, 1\}$ is a binary variable representing the operating state of the TCL c. The model parameters $M_1 = \exp(-\Delta T/(R_{th}C_{th})) \approx 1 - \Delta T/(R_{th}C_{th})$ and $M_2 = R_{th}\eta_{t,c}$ are constructed of thermal capacitance C_{th}, thermal resistance R_{th}, and the coefficient of performance $\eta_{t,c}$ of TCL c, where ΔT is the sampling time. It is shown in [36] that the aggregate non-linear discrete behavior Eq. (5) of TCLs can be accurately approximated by the following linear continuous state model:

$$\theta_{k,c}^{h} = M_1 \theta_{k,c}^{h-1} + (1 - M_1)(\theta_A - M_2 x_{k,c}^{h}) \quad (6)$$

Here, the consumption rate $x_{k,c}^{h}$ is a continuous variable instead of a binary input of $\{0, x_{k,c}^{rat}\}$. If we rewrite the equation in terms of the consumption rate we have:

$$x_{k,c}^{h} = \left[[\theta_{k,c}^{h} - M_1 \theta_{k,c}^{h-1}]/(1 - M_1) - \theta_A \right] / - M_2 \quad (7)$$

We can use the mechanism proposed in [37] to model the customers' thermal comfort level according to the ISO 7730 model and evaluate the parameters R_{th}, C_{th}, $\eta_{t,c}$, and $x_{k,c}^{h}$ using Monte-Carlo simulation method. It is well-known that according to the physical capacity characteristic of the TCL appliance c (declared by the producer company), its consumption rate $x_{k,c}^{h}$ is bounded between $x_{k,c}^{min}$ and $x_{k,a}^{max}$. On the other hand, knowing $\theta_{k,c}^{h-1}$ at the previous time slot $h - 1$ as an initial state for slot h and determining the desired temperature $\theta_{k,c}^{h}$ for that slot, the consumer k can set the proposer consumption rate $x_{k,c}^{h}$ for these high-flexible appliances $c \in \mathcal{A}_k^{hf}$ through (7). Based on the simplified model discussed in [38], the consumer k can evaluate/predict the thermal comfort conditions in moderate environments for his/her house. In this way, the consumer can effectively determine $\theta_{k,c}^{h}$ for all $h \in \mathcal{H}$, which consequently specifies the tolerable changes within energy bounds $E_{k,c}^{min}$ and $E_{k,a}^{max}$ (i.e., reducing parameters $[\theta_{k,c}^{h}]_{h\in\mathcal{H}}$ reduces the consumption rates $[x_{k,c}^{h}]_{h\in\mathcal{H}}$, which results in lowering the total energy consumption $E_{k,a}$ over the day, so, $E_{k,a} \neq E_{k,a}^{fix}$). Therefore, he/she could make a trade-off between reducing the cost and increasing the satisfaction level.

Most of the reported works in the literature assume that the customers are price-taker (i.e., the behavior of the active customers who participate in the DSM programs does not affect the electricity price signal) [39]. However, when there are a considerable number of active customers in the system, their power consumption behavior will be comparable to the conventional demand and inevitably influence the spot prices in the electricity market. Indeed, designing the price signal according to the price-taker assumptions results in creating sub-peaks/valleys jeopardizing the reliability and stability of the power system. So, it is essential provide a pricing policy in which the customers are considered to be price-participant, i.e., their consumption pattern affects the wholesale electricity price. Accordingly, inspired by the work in [40] and knowing that the marginal costs of supplying power forms some part of the effectual price p^h, we introduce the following real-time supply-bidding pricing policy for each slot h:

$$p^h = \tilde{p}_{bl}^{h}(\vartheta_1, \vartheta_2, \vartheta_3) + p_{sh}^{h}(\sum_{k\in\mathcal{K}} l_k^h) \quad (8)$$

where, the stochastic parameter $\tilde{p}_{bl}^{h}(\cdot)$ is the baseline real-time price which is not known to the customers and determined by the utility company, and $p_{sh}^{h}(\cdot)$ is the shadow price incurred due to the customers' regime of consumption. The utility company can manipulate the baseline price in order to guarantee its profit, according to the nature of the resources at hand. The shadow price is an increasing function of the total demand (e.g., $p_{sh}^{h} \cdot (\sum_{k\in\mathcal{K}} l_k^h)^2$) and makes sure that the load shifting by the customers to the low-price slots does not create other peaks. It is well-known that the baseline price signal $\tilde{p}_{bl}^{h}(\cdot)$ has usually the lowest amount at the valley of the total demand curve (when the aggregate power consumption is at the lowest level). We also know that the customers try to shift the operation time of their appliances to such slots. Therefore, adding the shadow price signal in (8) works as a regulator for the load-shifting behavior of the customers, reducing the fluctuation of the total system demand.

According to the utility theory [41], a legitimate utility function must be non-decreasing (i.e., the marginal benefit is non-negative) $\partial U(x, w)/\partial x \geq 0$, and the marginal benefit of each customer must be a non-increasing function $\partial^2 U(x, w)/\partial x^2 \leq 0$. Moreover, we assume that for a fixed consumption level x, a larger w gives a larger $U(x, w)$ (i.e., $\partial U(x, w)/\partial w > 0$), and when the consumption level is zero for all $w > 0$ we have $U(0, w) = 0$. The adopted utility function is as follows [42], [43]:

$$U_{k,a}^{h}(x_{k,a}^{h}, w_{k,a}^{h}) = \begin{cases} x_{k,a}^{h} \cdot w_{k,a}^{h} - \frac{\nu}{2}(x_{k,a}^{h})^2, & 0 \leq x_{k,a}^{h} < \frac{w_{k,a}^{h}}{\nu} \\ \frac{(w_{k,a}^{h})^2}{2\nu}, & x_{k,a}^{h} \geq \frac{w_{k,a}^{h}}{\nu} \end{cases} \quad (9)$$

where ν is a predetermined parameter and $w_{k,a}^{h}$ represents the preference (priority) of electricity consumption for appliance a of customer k at time slot h (e.g., higher $w_{k,a}^{h}$ means this appliance is willing to consume more power at slot h).

The integer variables in (1) make social welfare (4) a mixed-integer problem which is NP-hard in general. We can use the sequential quadratic programming (SQP) integrated with the Branch-and-Bound (B&B) method (such as the work in [44]) or Bender decomposition method (such as the work in [45]) to reduce the complexity of the problem. However, one can simply convert the integer variables into continuous variables. This method can reduce the computation time at the customers' side which is essential in our real-time DSM application. The idea is to decompose each consumption profile $\boldsymbol{X}_k \triangleq [\boldsymbol{x}_k^{in}, \boldsymbol{x}_k^{cn}]$ into vectors $\boldsymbol{x}_k^{in}$ with all integer and $\boldsymbol{x}_k^{cn}$ with all continuous variables. Subsequently, we replace each integer entry $0 \leq x_{k,a}^{h,in} \leq r_{k,a}^{u}$ of $\boldsymbol{x}_k^{in}$ with

This article has been accepted for publication in a future issue of this journal, but has not been fully edited. Content may change prior to final publication. Citation information: DOI 10.1109/JIOT.2020.2968539, IEEE Internet of Things Journal

its expansion $x_{k,a}^{h,in} := \{2^0 x_{k,a}^{h,0}, 2^1 x_{k,a}^{h,1}, \cdots, 2^v x_{k,a}^{h,v}\}$, where $v = \min\{(r-1)|2^r - 1 \geq r_{k,a}^u\}$ and $r_{k,a}^u$ is the upper bound of the integer variable $x_{k,a}^{h,in}$ [46]. We can let $x_{k,a}^{h,in} = x_{k,a}^{rat}$, $\forall h \in \mathcal{H}_{k,a}$ and take $x_{k,a}^{h,0} \in \{0,1\}$ as the decision variable at each slot h. Inspired by the work in [46], by introducing the following constraint we approximate all the integer variables as continuous variables:

$$x_{k,a}^{h,0} \cdot (1 - x_{k,a}^{h,0}) = 0, \; \forall a \in \mathcal{A}_k^{mf} \times \mathcal{A}_k^{lf}, h \in \mathcal{H}, k \in \mathcal{K} \quad (10)$$

As the interpretation of the corresponding integer variables in the DSM program is the power consumption rate of different electric appliances and the appliances can tolerate the consumption rate deviations lower than a Watt. This method provides good approximations of those integer variables, while is simple and has good coordination with the ADMM, augmentation-based penalty, and dual-decomposition techniques developed in the next section.

IV. Diffusion-ADMM Strategy

Without loss of generality, by letting $p_{sh}^h(\sum_{k\in\mathcal{K}} l_k^h) = p_{sh}^h \cdot (\sum_{k\in\mathcal{K}} l_k^h)^2$ for the price policy (8), and by assigning weight λ_k and multiplying -1 in (4), the following convex-continuous global incommodity minimization problem is defined:

$$\min_{\boldsymbol{X}} \mathcal{L}_1(\boldsymbol{X}) = \sum_{h\in\mathcal{H}} \sum_{k\in\mathcal{K}} \Big((1-\lambda_k)\big(\tilde{p}_{bl}^h + p_{sh}^h (\sum_{k\in\mathcal{K}} l_k^h)^2\big) l_k^h - \lambda_k \sum_{a\in\mathcal{A}_k} U_{k,a}^h(x_{k,a}^h, w_{k,a}^h) \Big), \; s.t. \; (1)-(3) \text{ and } (10) \quad (11)$$

where, we assume that each customer k determines a proper weight λ_k to make a trade-off between focusing on the cost minimization and utility maximization. In solving problem (11) in a fully distributed manner constraint (3) and shadow price $p_{sh}^h(\cdot)$ are challenging, because they spatially couple the solution among the customers. The goal of the DSM program is to minimize the overall power system cost including the power generation/transmission/distribution cost of the whole system (i.e., the first part of problem (11)) and the negative of the total utilities of all the customers (i.e., the second part of problem (11)). This structure of local costs of sub-systems plus shared common cost over the whole system is called the sharing problem [47]. One interesting and efficient solution to this sharing problem is the ADMM cost-sharing method [47].

Further, the need of providing the desired energy level for each appliance (presented in (1)), temporarily couples problem (11). So, each customer needs to know $\tilde{p}_{bl}^h$ for all $h \in \mathcal{H}$ to make an optimal decision. At first, to tackle constraint (3), we use dual-decomposition method as follows:

$$\min_{X} \mathcal{L}_2(\boldsymbol{X}, \boldsymbol{\mu}_u, \boldsymbol{\mu}_d) = \mathcal{L}_1(\boldsymbol{X}) + \sum_{h=1}^{H} \mu_u^h (\sum_{k\in\mathcal{K}} l_k^h - l^{max}) + \sum_{h=1}^{H} \mu_d^h (l^{min} - \sum_{k\in\mathcal{K}} l_k^h), \; s.t. \; (1), (2), \text{ and } (10) \quad (12)$$

with $\boldsymbol{\mu}_u \triangleq [\mu_u^h]_{h\in\mathcal{H}}$ and $\boldsymbol{\mu}_d \triangleq [\mu_d^h]_{h\in\mathcal{H}}$, where μ_u^h and μ_d^h are the Lagrangian multipliers at slot h for upper and lower bonds of constraint (3), respectively. Knowing optimal $\boldsymbol{\mu}_u$ and $\boldsymbol{\mu}_d$, $\mathcal{L}_1(\boldsymbol{X})$ is separable in terms of constraint (3) with the following dual problem:

$$\max_{\boldsymbol{\mu}_u, \boldsymbol{\mu}_d} \mathcal{D}(\boldsymbol{\mu}_u, \boldsymbol{\mu}_d) = \min_{X} \mathcal{L}_2(\boldsymbol{X}), \; s.t. \; (1), (2), \text{ and } (10) \quad (13)$$

However, problem (12) is still spatially-coupled due to the shadow price. Thus, we rewrite (12) as follows:

$$\min_{X} \mathcal{L}_2(\boldsymbol{X}) = \sum_{h\in\mathcal{H}} \Bigg(\sum_{k\in\mathcal{K}} \Big((1-\lambda_k)\cdot(\tilde{p}_{bl}^h \cdot l_k^h) - \lambda_k \cdot \sum_{a\in\mathcal{A}_k} U_{k,a}^h(x_{k,a}^h, w_{k,a}^h) \Big) + \mu_u^h (\sum_{k\in\mathcal{K}} l_k^h - l^{max}) + \mu_d^h (l^{min} - \sum_{k\in\mathcal{K}} l_k^h) \Bigg) + \underbrace{\sum_{h\in\mathcal{H}} \sum_{k\in\mathcal{K}} (1-\lambda_k)\cdot(p_{sh}^h \cdot l_k^h \cdot (\sum_{k\in\mathcal{K}} l_k^h)^2)}_{\text{I}},$$

$$s.t. \; (1), (2), \text{ and } [G_{k,g}(\boldsymbol{x}_k^{in}) = 0]_{g=1,\cdots,g_k}, \; \forall k \in \mathcal{K} \quad (14)$$

where $G_{k,g}(\boldsymbol{x}_k^{in})$ and g_k are the set of affine constraints and number of affine constraints of customer k, induced by integer constraints (10). Let $\mathcal{L}_2^I(\boldsymbol{X})$ denote part I of $\mathcal{L}_2(\boldsymbol{X})$ and $\mathcal{L}_2^{-I}(\boldsymbol{X})$ denote the rest. Now, using augmentation-based penalty methods we tackle the integer constraint complexity as follows [48]:

$$\min_{X} \mathcal{L}_3(\boldsymbol{X}) = \mathcal{L}_2^{-I}(\boldsymbol{X}) + \sum_{k\in\mathcal{K}} \eta_k . P_k(\boldsymbol{X}_k) + \mathcal{L}_2^I(\boldsymbol{X}), \quad s.t. \; (1) \text{ and } (2) \quad (15)$$

with penalty function associated with each customer $k \in \mathcal{K}$:

$$P_k(\boldsymbol{X}_k) \triangleq \sum_{g=1}^{g_k} \delta^{EP}(G_{k,g}(\boldsymbol{X}_k)), \; \delta^{EP}(x) = \begin{cases} 0, & x = 0 \\ > 0, & x \neq 0 \end{cases}$$

where P_k combines the affine constraints and is a smooth approximation to penalize the customer for assigning continuous variables to mid/low-flexible schedule of appliances. Moreover, the scalar parameter $\eta_k > 0$ is the penalty parameter and is used for controlling the relative importance of constraints (10), and $\delta^{EP}(\cdot)$ is the penalty function for the affine constraints (e.g., $\delta^{EP}(x) = x^2$).

Proposition 1. *The adopted penalty function $\delta^{EP}(x) = x^2$ is convex and $G_{k,g}(\boldsymbol{x}_k^{in})$ is affine. Therefore, each penalty term $\delta^{EP}(G_{k,g}(\boldsymbol{X}_k))$ becomes convex inducing the convexity of the aggregate penalty term $P_k(\boldsymbol{X}_k)$. On the other hand, the original objective function* (11) *(excluding the penalty term) is convex as it is composed of strictly convex cost function $C^h(\cdot)$, concave utility function $U_{k,a}^h$, and linear/affine constraints in* (1), (2), *and* (3)*. According to Theorem 1 in [48], when* (11) *is feasible, the minimizer of* (15) *will tend to the optimal solution of* (11) *as $\eta_k \to \infty$. Please refer to Chapter 9 of [49] for detailed analysis about the optimality of this mechanism and choosing appropriate η_k.*

The last step in the decomposition procedure is tackling part I of (14) using the ADMM. As a primal-dual optimization method, the ADMM technique has faster convergence than

This article has been accepted for publication in a future issue of this journal, but has not been fully edited. Content may change prior to final publication. Citation information: DOI 10.1109/JIOT.2020.2968539, IEEE Internet of Things Journal

primal domain alternatives, such as the gradient descent algorithm. Considering variable $\boldsymbol{X}_k$ as being the choice of customer k in the ADMM method; the sharing problem involves each customer adjusting its variable to minimize its individual part of independent costs $\mathcal{L}_2^{-I}(\boldsymbol{X}) + \sum_{k\in\mathcal{K}} \eta_k P_k(\boldsymbol{X}_k)$, as well as the shared objective term $\mathcal{L}_2^{I}(\boldsymbol{X})$. To resemble the classical sharing problem, let us rewrite the final unconstrained minimization problem as

$$\min_{\boldsymbol{X}} \mathcal{L}_3(\boldsymbol{X}) = \sum_{k\in\mathcal{K}} \mathcal{L}_3^{-I}(\boldsymbol{X}_k) + \mathcal{L}_2^{I}(\sum_{k\in\mathcal{K}} \boldsymbol{X}_k) \tag{16}$$

where $\sum_{k\in\mathcal{K}} \mathcal{L}_3^{-I}(\boldsymbol{X}_k) = \mathcal{L}_2^{-I}(\boldsymbol{X}) + \sum_{k\in\mathcal{K}} \eta_k P_k(\boldsymbol{X}_k)$, subject to local constraints (1) and (2), and $\mathcal{L}_2^{I}(\sum_{k\in\mathcal{K}} \boldsymbol{X}_k)$ is the shared objective. To decouple this shared objective, we write (16) in the ADMM form by substituting all the decision variables $\boldsymbol{X}_k$ for auxiliary variables in $\mathcal{L}_2^{I}(\sum_{k\in\mathcal{K}} \boldsymbol{X}_k)$:

$$\min_{\boldsymbol{X}_1,\cdots,\boldsymbol{X}_K} \sum_{k\in\mathcal{K}} \mathcal{L}_3^{-I}(\boldsymbol{X}_k) + \mathcal{L}_2^{I}(\sum_{k\in\mathcal{K}} \boldsymbol{Z}_k),\ s.t.\ \boldsymbol{X}_k - \boldsymbol{Z}_k = 0 \tag{17}$$

where $\boldsymbol{X}_k$ and $\boldsymbol{Z}_k$ have the same dimension. According to the ADMM theory the iterative solution of (17) with iteration index i takes the form [47]:

$$\begin{aligned}
\boldsymbol{X}_k^{i+1} &:= \arg\min_{\boldsymbol{X}_k} \Big(\mathcal{L}_3^{-I}(\boldsymbol{X}_k) + (\sigma/2)\left\|\boldsymbol{X}_k - \boldsymbol{Z}_k^i + \boldsymbol{U}_k^i\right\|_2^2\Big)\\
\boldsymbol{Z}_k^{i+1} &:= \arg\min_{\boldsymbol{Z}} \Big(\mathcal{L}_2^{I}(\sum_{k\in\mathcal{K}} \boldsymbol{Z}_k) + (\sigma/2)\sum_{k\in\mathcal{K}}\left\|\boldsymbol{Z}_k - \boldsymbol{U}_k^i - \boldsymbol{X}_k^{i+1}\right\|_2^2\Big)\\
\boldsymbol{U}_k^{i+1} &:= \boldsymbol{U}_k^i + \boldsymbol{X}_k^{i+1} - \boldsymbol{Z}_k^{i+1}
\end{aligned}$$

where $\boldsymbol{U}_k$ is the scaled dual variable and $\boldsymbol{Z}$-update at slot h requires solving a problem in $K\times(H-h+1)$ dimensional space. One method for adjusting parameter $\sigma > 0$ from iteration to iteration is to increase it until the iterative method used to carry out the updates converges quickly enough [47]. Let $\boldsymbol{V}_k^i = \boldsymbol{U}_k^i + \boldsymbol{X}_k^{i+1}$, to avoid the curse of dimensionality, let us rewrite the $\boldsymbol{Z}$-update as follows:

$$\min_{\boldsymbol{Z}_1,\cdots,\boldsymbol{Z}_K} \mathcal{L}_2^{I}(K\bar{\boldsymbol{Z}}) + (\sigma/2)\sum_{k\in\mathcal{K}}\left\|\boldsymbol{Z}_k - \boldsymbol{V}_k^i\right\|_2^2,\ s.t.\ \bar{\boldsymbol{Z}} = (1/K)\sum_{k\in\mathcal{K}} \boldsymbol{Z}_k \tag{18}$$

where the solution for each customer k is $\boldsymbol{Z}_k = \boldsymbol{V}_k^i + \bar{\boldsymbol{Z}} - \bar{\boldsymbol{V}}$ with $\bar{\boldsymbol{V}} = (1/K)\sum_{k\in\mathcal{K}} \boldsymbol{V}_k^i$, which converts (18) to unconstrained version $\min \mathcal{L}_2^{I}(K\bar{\boldsymbol{Z}}) + (\sigma/2)\sum_{k\in\mathcal{K}}\left\|\bar{\boldsymbol{Z}} - \bar{\boldsymbol{V}}\right\|_2^2$. Substituting in the solution expression for $\boldsymbol{Z}_k$ in the $\boldsymbol{U}$-update gives $\boldsymbol{U}_k^{i+1} := \bar{\boldsymbol{U}}^i + \bar{\boldsymbol{X}}^{i+1} - \bar{\boldsymbol{Z}}^{i+1}$ with $\bar{\boldsymbol{X}} = (1/K)\sum_{k\in\mathcal{K}} \boldsymbol{X}_k$. This shows that the dual variables $\boldsymbol{U}_k^{i+1}$ are all equal and can be replaced with a single dual variable $\boldsymbol{U}$. Finally, by substituting in the solution expression for $\boldsymbol{Z}_k$ in the $\boldsymbol{X}$-update, the relaxed algorithm becomes [47]:

$$\begin{aligned}
\boldsymbol{X}_k^{i+1} &:= \arg\min_{\boldsymbol{X}_k} \Big(\mathcal{L}_3^{-I}(\boldsymbol{X}_k) + (\sigma/2)\left\|\boldsymbol{X}_k - \boldsymbol{X}_k^i + \bar{\boldsymbol{X}}^i - \bar{\boldsymbol{Z}}^i + \boldsymbol{U}^i\right\|_2^2\Big)\\
\bar{\boldsymbol{Z}}^{i+1} &:= \arg\min_{\bar{\boldsymbol{Z}}} \Big(\mathcal{L}_2^{I}(K\bar{\boldsymbol{Z}}) + (K\sigma/2)\left\|\bar{\boldsymbol{Z}} - \boldsymbol{U}^i - \bar{\boldsymbol{X}}^{i+1}\right\|_2^2\Big)\\
\boldsymbol{U}^{i+1} &:= \boldsymbol{U}^i + \bar{\boldsymbol{X}}^{i+1} - \bar{\boldsymbol{Z}}^{i+1}
\end{aligned} \tag{19}$$

where the first step can be carried out independently in parallel at the customers side and the second and third steps at the utility company, which completes the optimization process.

For each customer k, to make an optimal decision, the knowledge about behavior of $\tilde{p}_{bl}^h$ for all upcoming slots $h\in\mathcal{H}$ is essential, while each of which is a stochastic scalar. The last part of the proposed mechanism is tackling the uncertainty of $\tilde{p}_{bl}^h$ by cooperatively estimate it using the diffusion-LMS strategy [50]. This method is scalable, robust, and imposes low communication/computation burden to the grid. Let d_k^h denote the payment imposed on customer k at slot h regarding the baseline price $\tilde{p}_{bl}^h$. Due to the stochastic nature of $\tilde{p}_{bl}^h$, customer k observes scalar d_k^h of some random process $\tilde{d}_k^h$ resulted from regression vector $\boldsymbol{u}_k^h = \tilde{\boldsymbol{l}}_k^h + \tilde{\boldsymbol{z}}_k^h$ where $\tilde{\boldsymbol{z}}_k^h$ are explanatory data available at each customer side. Without loss of generality, regressors $\boldsymbol{u}_k^h$ are assumed to be the demand profiles $\boldsymbol{l}_k^h \triangleq [l_k^h,\cdots,l_k^H] \in \mathbb{R}^{1\times(H-h+1)}$ from the previous slots and days updated at each slot only. However, one can incorporate other data (such as weather, fuel cost and change in other customers' behavior.) in the regressors to increase the estimation accuracy. To make an optimal decision for slot h, each customer $h\in\mathcal{K}$ should estimate the potential payment resulted for the rest of slots $(H-h)$, caused by the decision at slot h. So, we model the random process $\tilde{\boldsymbol{l}}_k^h$ from which $\boldsymbol{l}_k^h$ is drawn, which is correlated with $\tilde{d}_k^h$. The objective at each slot $h\in\mathcal{H}$ is for every customer in the grid to use its private data $\{d_k^h, \boldsymbol{l}_k^h\}$ to estimate price vector $\tilde{\boldsymbol{p}}_{bl}^h \triangleq [\tilde{p}_{bl}^h,\cdots,\tilde{p}_{bl}^H]^\top$ for $H-h+1$ slots. We consider the linear model for the customer k's observation/action as follows:

$$\tilde{d}_k^h = \tilde{\boldsymbol{l}}_k^h \tilde{\boldsymbol{p}}_{bl}^h + \tilde{v}_k^h \tag{20}$$

where, inaccuracy coefficient (noise) $\tilde{v}_k^h$ is a zero-mean random variable with variance $\sigma_{v,k}^2$, independent of $\tilde{\boldsymbol{l}}_k^h$ for all $k\in\mathcal{K}$ and h, and independent of $\tilde{v}_\ell^t$ for $\ell\neq k$ or $t\neq h$.

Assumption 1. *All regressors $[\tilde{\boldsymbol{l}}_k^h]_{k\in\mathcal{K},}^{h\in\mathcal{H}}$ are spatially and temporally independent, which is really true in the DSM setup as are decided based on the current price signal and the customers' desire.*

We say that two customers are connected if they can communicate directly with each other and we show the set of customers connected to customer k (including itself) by $\mathcal{N}_k$. The global LMS estimation problem is defined as follows:

$$J(\hat{p}_{bl}^h) \triangleq \sum_{k=1}^{K} \mathbb{E}\Big[|\tilde{d}_k^h - \tilde{\boldsymbol{l}}_k^h \tilde{\boldsymbol{p}}_{bl}^h|^2\Big] \tag{21}$$

However, the solution to this is not distributed and requires access to the data across the entire grid, which has several drawbacks (as mentioned in Section I). One can rewrite (21) as [50]:

$$\acute{J}(\hat{\boldsymbol{p}}_{bl}^h) \triangleq \sum_{\ell\in\mathcal{N}_k} c_{\ell,k}\mathbb{E}\Big[|\tilde{d}_\ell^h - \tilde{\boldsymbol{l}}_\ell^h \tilde{\boldsymbol{p}}_{bl}^h|^2\Big] + \sum_{\ell\neq k}^{K}\left\|\hat{\boldsymbol{p}}_{bl}^h - \hat{\boldsymbol{p}}_{bl,\ell}^h\right\|_{\Gamma_\ell}^2 \tag{22}$$

where $J_k(\cdot)$ is the estimation problem at customers k's side, $[c_{\ell,k}]_{\ell\in\mathcal{N}_k}$ are used to apply different weights to the neighbors' data, $\hat{\boldsymbol{p}}_{bl,\ell}^h$ is the local optimal solution for customer ℓ, and $\Gamma_\ell \triangleq \sum_{n\in\mathcal{N}_\ell} c_{n,\ell} R_{u,n}$ with $R_{u,n} = \mathbb{E}[\tilde{\boldsymbol{l}}_n^{h*}\tilde{\boldsymbol{l}}_n^h]$. To provide a fully distributed agent-based estimation mechanism, objective function (22) is approximated by the following modified

This article has been accepted for publication in a future issue of this journal, but has not been fully edited. Content may change prior to final publication. Citation information: DOI 10.1109/JIOT.2020.2968539, IEEE Internet of Things Journal

function:

$$J_k(\hat{\boldsymbol{p}}_{bl}^h) \triangleq \sum_{\ell\in\mathcal{N}_k} a_{\ell,k}\mathbb{E}\Big[|\tilde{d}_\ell^h - \tilde{\boldsymbol{l}}_\ell^h \tilde{\boldsymbol{p}}_{bl}^h|^2\Big] + \sum_{\ell\in\mathcal{N}_k/k}^{K} b_{\ell,k}\left\|\hat{\boldsymbol{p}}_{bl}^h - \hat{\boldsymbol{\varphi}}_{bl,\ell}^h\right\|^2 \quad (23)$$

where $\hat{\boldsymbol{\varphi}}_{bl,\ell}^h$ is the intermediate estimate of customer ℓ that is available at customer k and $b_{\ell,k}$ is its weight (see [51] for detailed analysis about the accuracy of this approximation). Minimizing problem (23) for estimating $\hat{\boldsymbol{p}}_{bl}^h$ at customer k denoted by $\hat{\boldsymbol{p}}_{bl,k}^{h,i}$ using a traditional iterative steepest-descent solution takes the following form [52]:

$$\begin{aligned}\hat{\boldsymbol{p}}_{bl,k}^{h,i} &= \hat{\boldsymbol{p}}_{bl,k}^{h,i-1} + \mu_k[\nabla_{\hat{\boldsymbol{p}}_{bl}^h} J_k(\hat{\boldsymbol{p}}_{bl}^h, i-1)]^* \\ &= \hat{\boldsymbol{p}}_{bl,k}^{h,i-1} + \mu_k \sum_{\ell\in\mathcal{N}_k} a_{\ell,k}(R_{du,\ell} - R_{u,\ell}\hat{\boldsymbol{p}}_{bl,k}^{h,i-1}) \\ &\quad + \nu_k \sum_{\ell\in\mathcal{N}_k/k} b_{\ell,k}(\hat{\boldsymbol{\varphi}}_{bl,\ell}^h - \hat{\boldsymbol{p}}_{bl,k}^{h,i-1}) \end{aligned} \quad (24)$$

where $R_{du,\ell} = \mathbb{E}[\tilde{d}_\ell^h \tilde{\boldsymbol{l}}_\ell^{h*}]$. The incremental technique [53], can improve the accuracy by iterating sequentially over each term of (24) with updating $\hat{\boldsymbol{p}}_{bl,k}^{h,i-1}$ and $\hat{\boldsymbol{\varphi}}_{bl,\ell}^h$ as follows:

$$\begin{aligned}\hat{\boldsymbol{\varphi}}_{bl,k}^{h,i} &= \hat{\boldsymbol{p}}_{bl,k}^{h,i-1} + \mu_k \sum_{\ell\in\mathcal{N}_k} a_{\ell,k}(R_{du,\ell} - R_{u,\ell}\hat{\boldsymbol{p}}_{bl,k}^{h,i-1}), \\ \hat{\boldsymbol{p}}_{bl,k}^{h,i} &= \hat{\boldsymbol{\varphi}}_{bl,k}^{h,i} + \nu_k \sum_{\ell\in\mathcal{N}_k/k} b_{\ell,k}(\hat{\boldsymbol{\varphi}}_{bl,\ell}^{h,i} - \hat{\boldsymbol{\varphi}}_{bl,k}^{h,i}) \\ &= (1-\nu_k+\nu_k b_{k,k})\hat{\boldsymbol{\varphi}}_{bl,k}^{h,i} + \nu_k \sum_{\ell\in\mathcal{N}_k/k} b_{\ell,k}\hat{\boldsymbol{\varphi}}_{bl,\ell}^{h,i} \end{aligned} \quad (25)$$

To adaptively estimate the cost in real-time we can replace $R_{du,\ell}$ and $R_{u,\ell}$ with their instantaneous approximations $R_{du,\ell} \approx d_\ell^{h,i}\boldsymbol{l}_\ell^{h,i^*}$ and $R_{u,\ell} \approx \boldsymbol{l}_\ell^{h,i^*}\boldsymbol{l}_\ell^{h,i}$. Finally, setting $c_{k,k} = 1-\nu_k+\nu_k b_{k,k}$ and $c_{k,\ell} = \nu_k b_{k,\ell}$ in (25), we reach the following adaptive diffusion adapt-then-combine (ATC) real-time price estimation method [50]:

Adaptation Step:

$$\hat{\boldsymbol{\varphi}}_{bl,k}^{h,i} = \hat{\boldsymbol{p}}_{bl,k}^{h,i-1} + \mu_k \sum_{\ell\in\mathcal{N}_k} a_{\ell,k}\boldsymbol{l}_\ell^{h,i^*}(d_\ell^{h,i} - \boldsymbol{l}_\ell^{h,i}\hat{\boldsymbol{p}}_{bl,k}^{h,i-1})$$

Combination Step:

$$\hat{\boldsymbol{p}}_{bl,k}^{h,i} = \nu_k \sum_{\ell\in\mathcal{N}_k} c_{\ell,k}\hat{\boldsymbol{\varphi}}_{bl,\ell}^{h,i} \quad (26)$$

where the weighting coefficients $\boldsymbol{A} = [a_{\ell,k}]_{\ell,k\in\mathcal{K}} \in \mathbb{R}^{K\times K}$ and $\boldsymbol{C} = [c_{\ell,k}]_{\ell,k\in\mathcal{K}} \in \mathbb{R}^{K\times K}$ are real, non-negative, and satisfy:

$$a_{\ell,k} = c_{\ell,k} = 0\; \forall \ell \notin \mathcal{N}_k, \mathbb{1}^\top\boldsymbol{A} = \mathbb{1}^\top, \boldsymbol{A}\mathbb{1} = \mathbb{1}, \mathbb{1}^\top\boldsymbol{C} = \mathbb{1}^\top \quad (27)$$

The diffusion ATC (26) is one kind of diffusion family; other kinds are with different orders and updating rules. However, the ATC is widely used due to its simplicity and better performance [54]. There are several rules to select adaptation, $[a_{\ell,k}]_{\ell,k\in\mathcal{K}}$, and combination, $[c_{\ell,k}]_{\ell,k\in\mathcal{K}}$, weights such as static selection according to the topology of the system (uniform or averaging rule [55], Metropolis rule [56], relative-degree rule [57], Laplacian rule [58], etc.), and dynamic selection (adaptive rule, relative variance rule, Hastings rule, etc.) [54], [59], [60]. The idea of the adaptive rules is, for example, if some customer k can determine which of its neighbors is less accurate in the price estimation. He can then assign smaller adaptation and combination weights to its interaction with that neighbor. As an insight, we introduce the adaptive relative variance rule for determining $c_{\ell,k}$ in which the customer determines the weights equal to the inverses of the noise variances of the neighbor's data as follows [61]:

$$c_{\ell,k} = \begin{cases} \frac{1}{\gamma_{\ell,k}^2}\big(\sum_{n\in\mathcal{N}_k}\frac{1}{\gamma_{n,k}^2}\big)^{-1} & \text{if } \ell\in\mathcal{N}_k \\ 0 & \text{otherwise} \end{cases} \quad (28)$$

with $\gamma_\ell^2 \triangleq \mu_\ell^2 \mathrm{tr}(G_\ell)$, where G_ℓ is the moment matrice. For real data this is equal to $R_{s,k}$ calculated as follows [54]:

$$R_{s,k} \triangleq \lim_{i\to\infty}\mathbb{E}[s_{k,i}(\tilde{\boldsymbol{p}}_{bl,k}^h)s_{k,i}^*(\tilde{\boldsymbol{p}}_{bl,k}^h)|\mathcal{F}_{i-1}] \quad (29)$$

where $s_{k,i}(\psi) \triangleq \hat{\nabla}_{\tilde{\boldsymbol{p}}_{bl,k}^{h*}} J_k(\psi) - \nabla_{\tilde{\boldsymbol{p}}_{bl,k}^{h*}} J_k(\psi)$, and $\mathcal{F}_{i-1}$ denotes the filtration corresponding to all past iterates across all the customers. To refrain curse of the computational complexity, one can use a simple iterative rule for learning $\gamma_{\ell,k}^{2,i}$ using a learning factor $\vartheta_c \in (0,1)$ as follows [59]:

$$\hat{\gamma}_{\ell,k}^{2,i} = (1-\vartheta_c)\hat{\gamma}_{\ell,k}^{2,i-1} + \vartheta_c\left\|\hat{\boldsymbol{\varphi}}_{bl,\ell}^{h,i} - \hat{\boldsymbol{p}}_{bl,k}^{h,i-1}\right\|^2 \quad (30)$$

In Section V we show that it has better performance in terms of the mean square deviation (MSD) measure, i.e., $MSD = 1/I\cdot\sum_{i=1}^{I}||\tilde{\boldsymbol{p}}_{bl}^h - \hat{\boldsymbol{p}}_{bl,k}^{h,i}||^2$. However, improving the estimation performance in terms of MSD comes at the expense of deterioration in the convergence speed during the transient phase of the estimation process (26) [60]. It is suggested that the customers at first use a fixed combination rule (as we used Metropolis rule in [34]) and then switch to dynamic combination rule (28) [59].

Remark 2. The network topology does not influence the performance of the system and the only important thing is that the network topology must be a connected-graph [62]. As it is shown in [50], adaptive diffusion LMS estimation strategy (26) with data model (20) and Assumption 1 is asymptotically unbiased for any initial condition and any choice of matrices $\boldsymbol{A}$ and $\boldsymbol{C}$ satisfying (27) if, and only if,

$$0 < \mu_k < \frac{2}{\lambda^{max}(\sum_{\ell\in\mathcal{K}} a_{\ell,k}R_{u,\ell})}, \forall k\in\mathcal{K}$$

where $\lambda^{max}(\cdot)$ is the maximum eigenvalue of a Hermitian matrix.

At the end of each slot h, the utility company reveals the price parameters $\tilde{p}_{bl}^h$ and p_{sh}^h, the cost imposed by it, and the total system consumption at that slot. If explanatory variables (e.g., $\tilde{\boldsymbol{z}}_k^h$) are provided to help the customers making more accurate estimation, the utility company can also update that variables and send them to the customers. Accordingly, the customers update their information and constraints (1) and (2), and apply again the estimation and optimization tools under the (event-triggered) MPC protocol to increase

This article has been accepted for publication in a future issue of this journal, but has not been fully edited. Content may change prior to final publication. Citation information: DOI 10.1109/JIOT.2020.2968539, IEEE Internet of Things Journal

Algorithm 1 Diffusion-ADMM DSM Mechanism

I. **Initialization:** Set an optional profile $\boldsymbol{X}_k \in \mathbb{R}^{H \times A_k}$, the baseline price signal $\tilde{\boldsymbol{p}}_{bl}^0 \in \mathbb{R}^{H \times 1}$, and ϵ_1, ϵ_2.
II. **Repeat** for $h = 1, 2, \cdots, H$:
  Estimation Phase: Set initial values for $\hat{\boldsymbol{p}}_{bl,k}^{h,0}$.
    Iterate for $i = 1, 2, \cdots$:
      Receive predicted payment $d_\ell^{h,i} \in \mathbb{N}$ and scheduled aggregate demand profile $\boldsymbol{l}_\ell^{h,i} \in \mathbb{R}^{1 \times (H-h+1)}$ from all neighbors $\ell \in \mathcal{N}_k$.
      Run estimation iterations (26).
      Update adaptation, $[a_{\ell,k}]_{\ell \in \mathcal{N}_k}$, and combination, $[c_{\ell,k}]_{\ell \in \mathcal{N}_k}$ weights, e.g., through (28).
    Until convergence (i.e., $\left\| \hat{\boldsymbol{p}}_{bl,k}^{h,i+1} - \hat{\boldsymbol{p}}_{bl,k}^{h,i} \right\| \leq \epsilon_1$)
  Optimization Phase: Utility company set initial values for $\bar{\boldsymbol{X}}^0, \bar{\boldsymbol{Z}}^0, \boldsymbol{U}^0 \in \mathbb{R}^{H \times A_k}$..
    Iterate for $i = 1, 2, \cdots$:
      Receive updated $\bar{\boldsymbol{X}}^i$, $\bar{\boldsymbol{Z}}^i$, and $\boldsymbol{U}^i$ from the utility company.
      Run first line of (19) and update the consumption profile $\boldsymbol{X}_k^i \rightarrow \boldsymbol{X}_k^{i+1}$.
      If $\left\| \boldsymbol{X}_k^{i+1} - \boldsymbol{X}_k^i \right\| \geq \epsilon_2$ (i.e., the new schedule changes compared to the current schedule),
      Then set $\boldsymbol{X}_k^{i+1}$ as the new solution and broadcast it to the utility company.
      The utility company receives all $[\boldsymbol{X}_k^{i+1}]_{k \in \mathcal{K}}$ and updates $\{\bar{\boldsymbol{X}}^i, \bar{\boldsymbol{Z}}^i, \boldsymbol{U}^i\} \rightarrow \{\bar{\boldsymbol{X}}^{i+1}, \bar{\boldsymbol{Z}}^{i+1}, \boldsymbol{U}^{i+1}\}$ using the second and third lines of (19).
    Until convergence (i.e., none of the customers broadcast their schedules and updated information)
  Customer k applies the first row of matrix $\boldsymbol{X}_k$ and discards the others according to the MPC protocol (e.g., [63]).
  The utility company reveals true values for $\tilde{p}_{bl}^h$ and $\sum_{k \in \mathcal{K}} l_k^h$, and customer k updates explanatory variables $\tilde{\boldsymbol{z}}_k^h$, at the end of time-slot h.

the DSM's performance [63]. To better demonstrate the data communication/computation and the customers' interactions in the proposed framework, the whole Diffusion-ADMM based DSM structure is shown in Algorithm 1.

V. Numerical Results

The simulation environment is MATLAB R2017b run on a PC Laptop 64-bit Intel(R) Core(TM) i7-4510U CPU @2.00-2.60GHz RAM 8.00GB. For the simulation set-up we have used real-time price signal data from 5/05/2019 to 5/09/2019 of two pricing mechanisms (five-minute-based and hourly-based) for pricing node ID 1 (PJM-RTO zone) of Pennsylvania-New Jersey-Maryland Interconnection (PJM) electricity market [64]. For the real-time performance analysis of our diffusion price estimation mechanism, we have adopted a five-minute-based price signal at 5/05/2019 of the PJM-RTO zone as the reference signal and applied the proposed mechanism to estimated it. The result is shown in Fig. 1, which denotes the efficiency of the proposed cooperative mechanism.

The diffusion-LMS price estimation algorithm with different rules is evaluated in Fig. 2 to denote the robustness of the algorithm. In this figure, as the reference, we have considered the hourly-based real-time electricity price data from PJM-RTO zone at 5/06/2019. To model the effect of customers' behavior in scheduling their consumption pattern with the proposed ADMM DSM approach on the price market in the considered day, we assume that the price behavior has the mean equal to the reference price with some variation with a uniform distribution around it (i.e., a white Gaussian noise). The estimation performance of each customer is modeled with

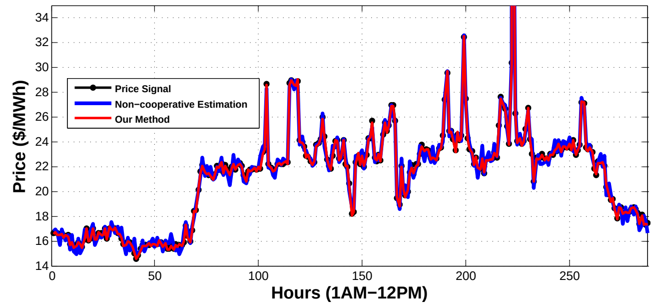

Fig. 1. Diffusion LMS-based price estimation for five-minute real-time PJM market price.

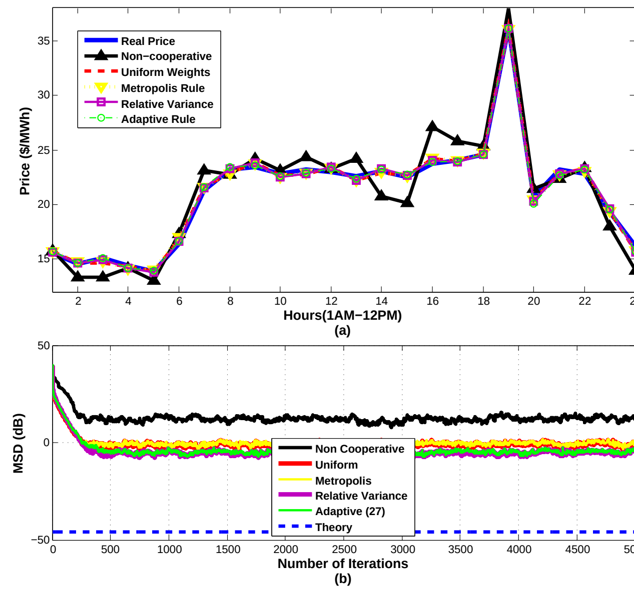

Fig. 2. Diffusion LMS-based price estimation; a) estimation accuracy comparison and b) MSD performance evaluation.

a benchmark minimum noise power between -30 and -10dB plus a random uniform distributed accumulated noise variance between 10 $\tilde{\upsilon}_k^h$ and 50 $\tilde{\upsilon}_k^h$ incorporating the customers' characteristics. Fig. 2(a) denotes the estimation performance over the real price and Fig. 2(b) denotes the estimation performance evaluation in terms of the MSD measure. In non-cooperating method there is not any data sharing between the customers, in uniform method each customer assigns equal weights $a_{\ell,k}$ and $c_{\ell,k}$ to each neighbor's data. Metropolis method assigns the weights according to the degree (i.e., the number of neighbors) of each customer. Evidently, all the cooperative methods result in better estimation compared with non-cooperative ones, while, relative variance rule (28) is the most accurate among all.

The comparison between three DSM scenarios in which constraint (3) is not considered (called No Bound), there is no cost-sharing like pricing policy (8) (called Static Price), and the proposed framework is depicted in Fig. 3. In the No Bound case, the total system consumption is not bounded. So, the customers try to consume more energy at slots with low price and less (or negative) energy at high price slots to reduce their payments as much as possible. However, they do not

This article has been accepted for publication in a future issue of this journal, but has not been fully edited. Content may change prior to final publication. Citation information: DOI 10.1109/JIOT.2020.2968539, IEEE Internet of Things Journal

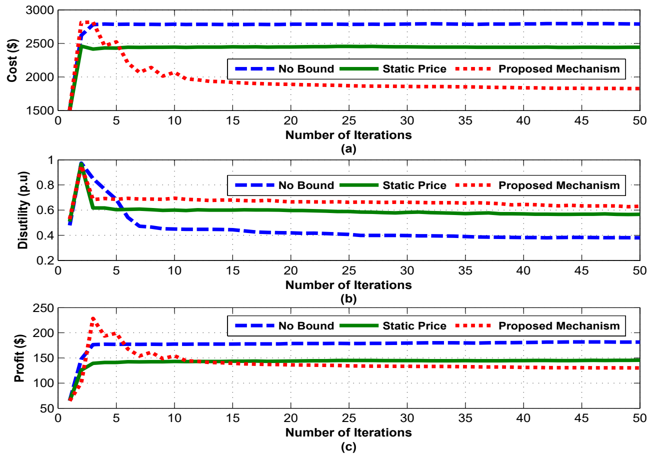

Fig. 3. Result comparison between three DSM scenarios; a) Aggregated customers' payment, b) aggregate customers' utility level (9), and c) The utility company's profit.

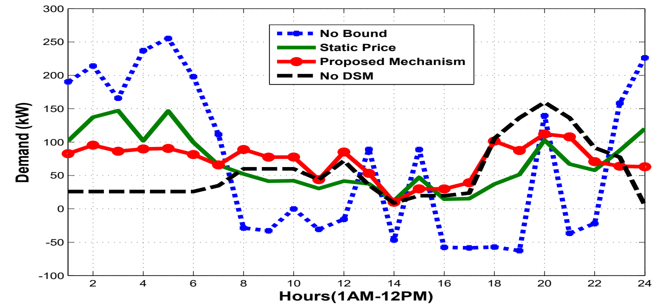

Fig. 4. The aggregated system's load curves in different scenarios.

know that their behavior results in more fluctuations in the load curve which subsequently changes the price signal, resulting in more payment as shown in Fig. 3(a). Without iterative ADMM method (19) in the Static Price case, the payment is reduced. However, as they are not provided by the energy cost-sharing mechanism and the customers do not have the shadow price function and the information about the total consumption of the other customers, their behavior still incurs more shadow price to them.

In the case where there is no DSM program, the customers use their appliances once needed resulting in the highest utility level (maximum amount for (9)). However, any deviation from this situation results in some dissatisfaction which justifies Fig. 3(b) where the No Bound case achieves the minimum disutility (discomfort) level. As denoted, our method, although applies more limitation to the customer actions, results in the lowest payment. From this result, we can conclude that there is no ideal strategy which results is the lowest payment and the highest satisfaction (utility) level. So, the customers always have to make a trade-off between operating their appliances whenever they need (increasing the satisfaction level) and changing their operation time and/or the amount of power consumption in order to reduce the payment.

The result of Fig. 3(c) is challenging, it seems the utility company can cheat and earns more profit by providing less information (about the price parameters, the peak time, and the dual-decomposition and ADMM multipliers) to the customers. However, increasing the peak demand and the load curve fluctuation would significantly increase the supply cost (the cost of buying power from the wholesale electric market, the operational and taxes costs, the self-generated power cost, etc.). So, the possibility of cheating by the utility company can be tackled by an appropriate selection of the wholesale market price $C^h(\cdot)$ and other taxes policies.

In another view, deliberately or inadvertently providing false or imperfect data significantly reduces the DSM performance as shown in Fig. 4. We can see in this figure that in the No Bound case (i.e., without considering constraint (3) and the proposed pricing policy (8)) the sub-peak created in low time slots is even bigger than the original peak. As denoted, the customers have tried to sell electricity back to the grid in some time-slots. Also this high amount of reverse current has adverse effect on the reliability and power quality of the power grid, which results in a high penalty cost for the utility company and the customers. Moreover, for the Static Price case we can see that the demand curve still has high fluctuations. These fluctuations reduce the customer satisfaction, increase the power distribution loss (as the power flow through the lines deviated from the determined optimal power flow (OPF)), and can increase the cost of ancillary serves for increasing the power quality. However, when there is a shadow price $p_{sh}^h(\cdot)$ (the proposed mechanism case), the customers' aggregate consumption behavior tends to flat the total demand curve to refrain suffering from both high baseline and shadow prices in (8). The common peak-to-average ratio (PAR) measure $PAR = H\max\{[l^h]_{h\in\mathcal{H}}\}/\sum_{h\in\mathcal{H}} l^h$ is; 2.9374 for No DSM, 3.0707 for No Bound, 1.7634 for Static Price, and 1.5130 for our framework.

According to the constraints in (1), the aggregated energy consumption must be equal for all appliances in all the scenarios during one scheduling horizon (their tasks must be fulfilled at the end of scheduling horizon $\mathcal{H}$). However, for the No DSM case, there is not any storage device, as there is no plan for it. On the other hand, in the Proposed Mechanism case, the customers start the DSM with empty[2] storage devices and end up with having full batteries at the end of $\mathcal{H}$. They can either sell all the energy stored in the batteries or save it for a better situation in the next scheduling horizon. In Fig. 4, the storage devices for the Proposed Mechanism case are not empty at the end of the scheduling horizon. Therefore, the aggregate energy consumption is more than the other cases.

The convergence of the proposed dual-decomposition-ADMM mechanism in terms of the multipliers is evaluated in Fig. 5. Figs. 5(a) and (b) show that once the consumption pattern of the customers tend to violate the supply capacity (i.e., constraint (3)), the penalties $\boldsymbol{\mu}_u$ and $\boldsymbol{\mu}_d$ increase to prevent that. As long as the DSM algorithm is running online, the customers' operations can violate constraint (3) and the utility company needs to continuously update the Lagrange multipliers $\boldsymbol{\mu}_u, \boldsymbol{\mu}_d$. This is why Figs. 5(a) and (b) have

[2]One can constraint the storage device energy level to be equal at the start and end of the scheduling horizon (i.e., set $E_{k,b}^0 = E_{k,b}^H$). In this case, the net energy consumption by the storage devices will be equal for both DSM and No DSM scenarios.

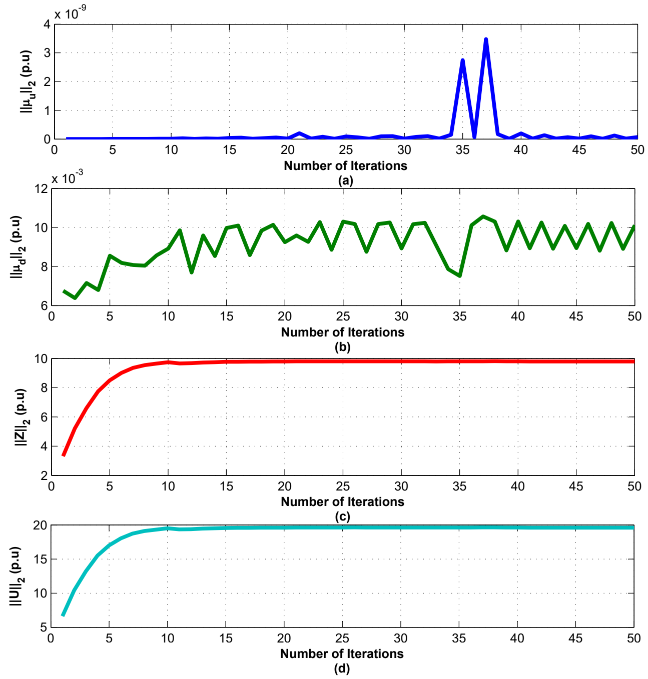

Fig. 5. Convergence of the proposed dynamic pricing mechanism in terms of the multipliers' norm; a) Lagrangian multiplier $\boldsymbol{\mu}_u$ corresponds to the upper bound l^{max} in constraint (3), b) Lagrangian multiplier $\boldsymbol{\mu}_d$ corresponds to the lower bound l^{min} in constraint (3), c) multiplier $\bar{\boldsymbol{Z}}$ of cost-sharing mechanism (19), and d) scaled dual variable $\boldsymbol{U}$ of cost-sharing mechanism (19).

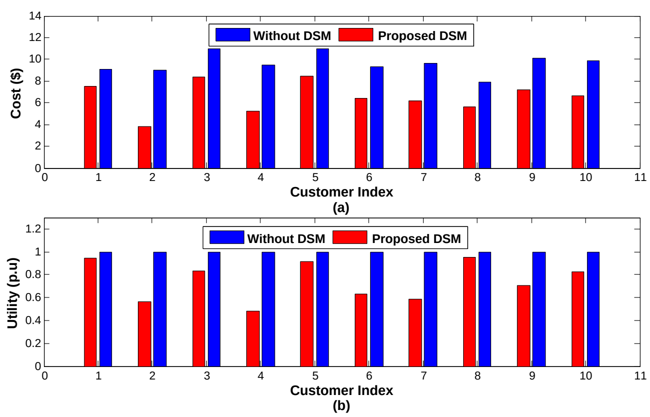

Fig. 6. Evaluation of the customer's motivations in terms of a) the payment reduction and b) confirmation of the utility level.

continuous oscillations. Figs. 5(c) and (d) justify the need for establishing an energy cost-sharing model by a dynamic pricing method. By this protocol as the customers' aggregate power consumption in some slots increases, the shadow prices are increased through the increase in $\bar{\boldsymbol{Z}}$ and $\boldsymbol{U}$.

Each customer's payment under our proposed mechanism is presented in Fig. 6(a) and its normalized utility (satisfaction) level is demonstrated in Fig. 6(b). From this result, we can claim that all the customers have the tendency to participate in the proposed mechanism. However, the comparison between Figs. 6(a) and (b) reveals that each customer needs to make a trade-off between more reducing the payment and less reducing the utility level by choosing a proper value for λ_k.

Another simulation is carried out to analyze the computa-

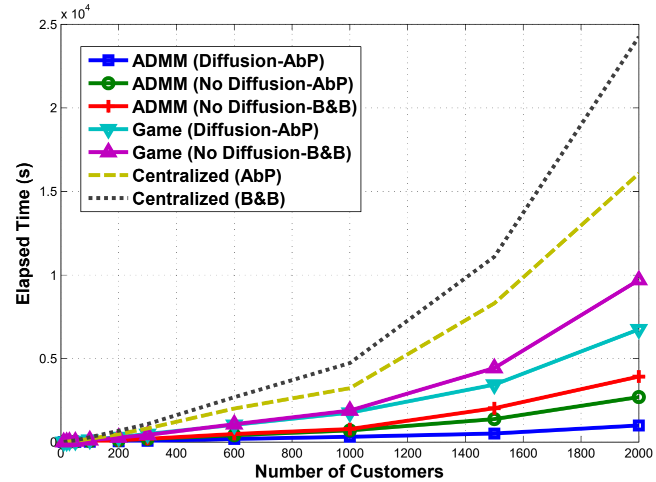

Fig. 7. Performance of the proposed mechanism in comparison with the other methods in terms of the total computation time unit convergence.

tional burden our method imposes to the system and compare it with the other potential methods. It is worth mentioning that methods like combining game theoretic strategy with Diffusion and AbP strategies (i.e., Game (Diffusion-AbP)) and ADMM strategy with AbP strategy (ADMM (No Diffusion-AbP)) are also proposed for the first time in the DSM literature. According to the depicted results in Fig. 7 we can see that performing the DSM mechanism in a centralized manner (such as [65]) imposes the most computational burden to the system. Note that the MIP technique is based on the B&B methods (i.e., the "Centralized (B&B)" case). When we use our continuous approximation AbP technique to lower the complexity of the MIP (i.e., the "Centralized AbP" case), the computational burden is significantly reduced. However, in the centralized methods the elapsed time to converge is not yet practical in the real world-real-time applications.

Other state of the art strategies in the DSM literature are game theoretic methods such as the well-known mechanism first introduced in [32]. In the game theoretic methods two factor can slow down the convergence speed; 1) It is necessary for each customer to know the aggregated consumption of all the other customers and decide accordingly (imposing high communication burden and time delay). 2) Simultaneously running the optimizations algorithm by the customers can result in a non-optimal solution [32]. However, as denoted by the case "Game (Diffusion-AbP)" when our diffusion price estimation is added to the game theoretic methods, the computation time is reduced. As shown in Fig. 7, it still takes more time tachieve the solution for the game-theoretic methods compared with the ADMM based methods. When we do not apply the diffusion strategy in our ADMM mechanism (i.e., "ADMM (No Diffusion-AbP)" and "ADMM (No Diffusion-B&B)"), the elapsed time to convergence are increase significantly.

The most important factor for the system participants, is the aggregate power cost. To compare our proposed mechanism with the other methods in this term, we provided another simulation its results is shown in Fig. 8. The considered

This article has been accepted for publication in a future issue of this journal, but has not been fully edited. Content may change prior to final publication. Citation information: DOI 10.1109/JIOT.2020.2968539, IEEE Internet of Things Journal

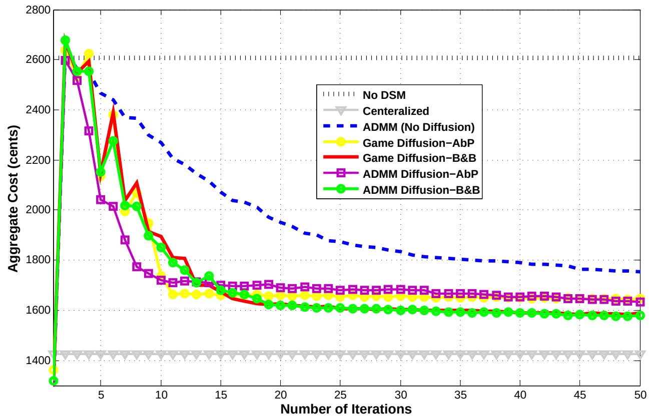

Fig. 8. Performance of the proposed mechanism in comparison with the other methods in terms of the aggregate system payment.

scenarios in this figure are as follows;

a) The “No DSM” case in which the customers operate their appliances at the nominal rate and consume power once they need. b) Our proposed mechanism, namely, the case “ADMM Diffusion-AbP”. c) The proposed method without the diffusion strategy for the estimation stage (i.e., the case “ADMM (No Diffusion)”), the aggregate system cost is increased as the customers estimated the price less accurately. d) The case “Game DiffusionAbP” denotes the scenario in which the optimization stage is performed through the game theory and the estimation stage through the proposed diffusion strategy. It seems that this scenario converges faster than the ADMM method. However, from Fig. 7, it takes more time for the game theoretic methods to perform each stage (as they are not allowed to perform simultaneously) while it is necessary for the customers to reach to an optimal solution and then broadcast their solution to the other customers. e) Combining the methods with the well-known B&B algorithm (the cases “ADMM Diffusion-B&B” and “Game Diffusion-B&B”). In these cases the B&B method is used for optimization part instead of converting the constrained problem into an unconstrained version and converting the integer variables into continuous ones. As depicted, the B&B method is more efficient, however, from Fig. 7 it imposes more computational burden on the system and is not suitable for a real-time DSM implementation. The results show that the centralized methods achieve the lowest electricity consumption cost. However, they are not scalable, impose a huge computational burden to the system, are not robust or secure to the communication failures, and the privacy of the customers in these methods are always at risk [34]. We can see that our framework achieves a sub-optimal aggregate cost same as those by the game theoretic method, but in a faster, more privacy preserving, and more scalable and robust manner.

The performance of the proposed mechanism when the data is corrupted (either deliberately by cheating or unintentional because of communication failures) is analyzed and the results are shown in Figs. 9 (a) and (b). The aggregate power consumption pattern in different scenarios are depicted in Fig. 9 (a). In this figure, the cases Cheat-Failure (optimization) and Cheat-Failure (estimation) denote the scenarios at which there is a perturbation affecting the interactions and corrupting the data at optimization and estimation stages, respectively. As denoted, in the perfect scenario of our framework (i.e., case No Cheat-Failure), the customers try to consume low power at high-power demand slot. This is because they effectively predict that both the price parameters $\tilde{p}_{bl}^h$ and $p_{sh}^h(\cdot)$ are high at that slot. This behavior significantly reduces the customers' payment (denoted in Fig. 9 (b)) and results in the lowest average PAR value of 1.1273, while the PAR of the No DSM case is 2.3601.

However, when some customers cheat and provide false information to their neighbors about the baseline price signal $\tilde{p}_{bl}^h$ and explanatory variables $\tilde{\boldsymbol{z}}_k^h$, the customers' payment are increased compared to the perfect scenario and the average PAR in this scenario is 1.4327. As each customer uses a learning mechanism (similar to (30)) to determined the value of information coming from its neighbors, the faulty customers are soon will be identified, punished, and disconnected from the network by setting $c_{\ell,k} = 0$. This is why the proposed mechanism is robust to communication/node failures.

From consumption behavior of the customers in Fig. 9 (a), case Cheat-Failure (estimation), we can see that the customers' peak demand coincides with the No DSM case. This is because the customers do not know that the price is the highest at theses slots, and consume more power to increase their utility through maximizing function (9).

The last scenario is when there are faulty agents providing fault data in the optimization stage (e.g., some customers consume more power than the quantity they declare to the utility company). This behavior significantly affects price parameter $p_{sh}^h(\cdot)$ and Lagrange multipliers $\boldsymbol{\mu}_u, \boldsymbol{\mu}_d$ due to the false information about quantity $\sum_{k\in\mathcal{K}} l_k^h$. From consumption behavior of the customers in Fig. 9 (a), case Cheat-Failure (optimization), we can see that the customers are trying to consume much power at low-price slot and low power at high-price slots, unaware of all other customers are trying the same. So, the customers payment are increased due to the growth of the shadow price and the penalty of violating constraint (3) and the average PAR increases to 1.6214.

VI. Conclusions

Here, a scalable robust DSM approach for smart grid including two sequentially repeated estimation and optimization parts has been investigated. For the first time, in the estimation part, we used a robust powerful diffusion-LMS strategy by which the customers estimate the price signal in a cooperative and decentralized manner. To optimize the system, a novel supply-bidding pricing policy has been introduced, a dual-decomposition method used to tackle the supply capacity limits. Also, an ADMM energy cost-sharing strategy developed to prevent any significant load fluctuations and creation of sub-peaks. Due to the mid/low flexible appliance characteristics, the proposed DSM mechanism must be formulated as a mixed-integer optimization problem which is computationally NP-hard. So, we converted the integer variables into continuous variables using the simple expansion approximation and augmentation-based penalty methods.

This article has been accepted for publication in a future issue of this journal, but has not been fully edited. Content may change prior to final publication. Citation information: DOI 10.1109/JIOT.2020.2968539, IEEE Internet of Things Journal

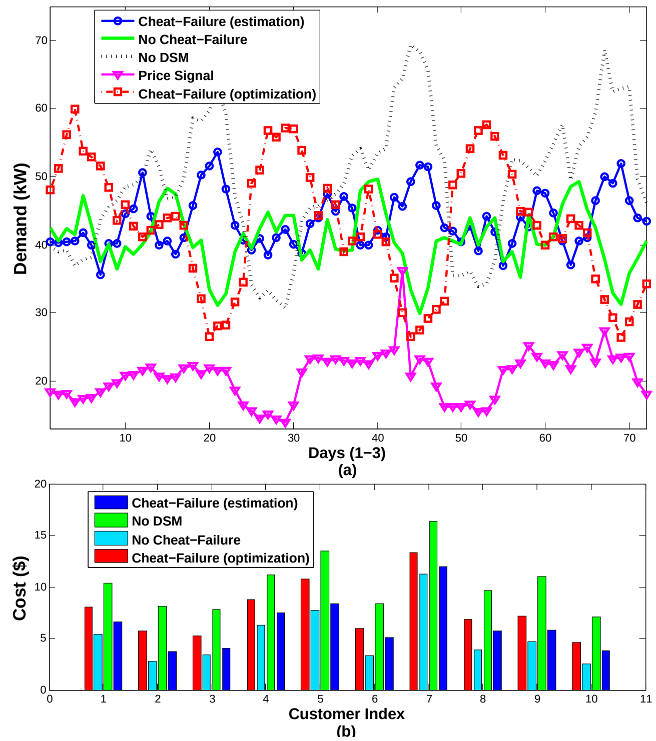

Fig. 9. Performance analysis of the proposed mechanism in the presence of communication failure and customer cheating.

Numerical simulations have demonstrated that the proposed framework has acceptable price estimation accuracy, imposes low communication/computational burden on the system, and reduces the load demand fluctuations significantly.

REFERENCES

[1] W. Chiu, H. Sun, and H. V. Poor, "Energy imbalance management using a robust pricing scheme," *IEEE Transactions on Smart Grid*, vol. 4, no. 2, pp. 896–904, June 2013.

[2] L. Barbierato, A. Estebsari, E. Pons, M. Pau, F. Salassa, M. Ghirardi, and E. Patti, "A distributed iot infrastructure to test and deploy real-time demand response in smart grids," *IEEE Internet of Things Journal*, vol. 6, no. 1, pp. 1136–1146, Feb 2019.

[3] T. Chiu, Y. Shih, A. Pang, and C. Pai, "Optimized day-ahead pricing with renewable energy demand-side management for smart grids," *IEEE Internet of Things Journal*, vol. 4, no. 2, pp. 374–383, April 2017.

[4] Y. Wang, S. Mao, and R. M. Nelms, "Distributed online algorithm for optimal real-time energy distribution in the smart grid," *IEEE Internet of Things Journal*, vol. 1, no. 1, pp. 70–80, Feb 2014.

[5] C. O. Adika and L. Wang, "Autonomous appliance scheduling for household energy management," *IEEE Transactions on Smart Grid*, vol. 5, no. 2, pp. 673–682, 2014.

[6] M. Ashabani and H. B. Gooi, "Multiobjective automated and autonomous intelligent load control for smart buildings," *IEEE Transactions on Power Systems*, vol. 33, no. 3, pp. 2778–2791, May 2018.

[7] F. Luo, G. Ranzi, C. Wan, Z. Xu, and Z. Y. Dong, "A multistage home energy management system with residential photovoltaic penetration," *IEEE Transactions on Industrial Informatics*, vol. 15, no. 1, pp. 116–126, Jan 2019.

[8] S. Faddel and O. A. Mohammed, "Automated distributed electric vehicle controller for residential demand side management," *IEEE Transactions on Industry Applications*, vol. 55, no. 1, pp. 16–25, Jan 2019.

[9] C. P. Mediwaththe, M. Shaw, S. K. Halgamuge, D. Smith, and P. M. Scott, "An incentive-compatible energy trading framework for neighborhood area networks with shared energy storage," *IEEE Transactions on Sustainable Energy*, pp. 1–1, 2019.

[10] Y. Du, J. Wu, S. Li, C. Long, and S. Onori, "Coordinated energy dispatch of autonomous microgrids with distributed mpc optimization," *IEEE Transactions on Industrial Informatics*, pp. 1–1, 2019.

[11] S. Althaher, P. Mancarella, and J. Mutale, "Automated demand response from home energy management system under dynamic pricing and power and comfort constraints," *IEEE Transactions on Smart Grid*, vol. 6, no. 4, pp. 1874–1883, 2015.

[12] S. Moon and J. Lee, "Multi-residential demand response scheduling with multi-class appliances in smart grid," *IEEE Transactions on Smart Grid*, vol. 9, no. 4, pp. 2518–2528, July 2018.

[13] F. Elghitani and W. Zhuang, "Aggregating a large number of residential appliances for demand response applications," *IEEE Transactions on Smart Grid*, vol. 9, no. 5, pp. 5092–5100, Sep. 2018.

[14] M. Latifi, A. Rastegarnia, A. Khalili, V. Vahidpour, and S. Sanei, "A distributed game-theoretic demand response with multi-class appliance control in smart grid," *Electric Power Systems Research*, vol. 176, p. 105946, 2019.

[15] K. Ma, Y. Yu, B. Yang, and J. Yang, "Demand-side energy management considering price oscillations for residential building heating and ventilation systems," *IEEE Transactions on Industrial Informatics*, pp. 1–1, 2019.

[16] A. Karapetyan, S. K. Azman, and Z. Aung, "Assessing the privacy cost in centralized event-based demand response for microgrids," in *Trustcom/BigDataSE/ICESS, 2017 IEEE*. IEEE, 2017, pp. 494–501.

[17] N. Li, L. Chen, and S. H. Low, "Optimal demand response based on utility maximization in power networks," in *Power and Energy Society General Meeting, 2011 IEEE*. IEEE, 2011, pp. 1–8.

[18] H. Farhangi, "The path of the smart grid," *IEEE power and energy magazine*, vol. 8, no. 1, 2010.

[19] S. Tsai, Y. Tseng, and T. Chang, "Communication-efficient distributed demand response: A randomized admm approach," *IEEE Transactions on Smart Grid*, vol. 8, no. 3, pp. 1085–1095, May 2017.

[20] ——, "Communication-efficient distributed demand response: A randomized admm approach," *IEEE Transactions on Smart Grid*, vol. 8, no. 3, pp. 1085–1095, May 2017.

[21] Y. Wang, L. Wu, and S. Wang, "A fully-decentralized consensus-based admm approach for dc-opf with demand response," *IEEE Transactions on Smart Grid*, vol. 8, no. 6, pp. 2637–2647, Nov 2017.

[22] M. H. K. Tushar, A. W. Zeineddine, and C. Assi, "Demand-side management by regulating charging and discharging of the ev, ess, and utilizing renewable energy," *IEEE Transactions on Industrial Informatics*, vol. 14, no. 1, pp. 117–126, Jan 2018.

[23] M. Latifi, A. Rastegarnia, A. Khalili, W. M. Bazzi, and S. Sanei, "A self-governed online energy management and trading for smart micro/nano-grids," *IEEE Transactions on Industrial Electronics*, pp. 1–1, 2019.

[24] Z. Cao, J. Lin, C. Wan, Y. Song, Y. Zhang, and X. Wang, "Optimal cloud computing resource allocation for demand side management in smart grid," *IEEE Transactions on Smart Grid*, vol. 8, no. 4, pp. 1943–1955, July 2017.

[25] M. H. Yaghmaee, M. Moghaddassian, and A. Leon-Garcia, "Autonomous two-tier cloud-based demand side management approach with microgrid," *IEEE Transactions on Industrial Informatics*, vol. 13, no. 3, pp. 1109–1120, 2017.

[26] N. Ahmed, M. Levorato, and G. P. Li, "Residential consumer-centric demand side management," *IEEE Transactions on Smart Grid*, vol. 9, no. 5, pp. 4513–4524, Sep. 2018.

[27] Z. Baharlouei, H. Narimani, and M. Hashemi, "On the convergence properties of autonomous demand side management algorithms," *IEEE Transactions on Smart Grid*, vol. 9, no. 6, pp. 6713–6720, Nov 2018.

[28] C. Li, X. Yu, W. Yu, G. Chen, and J. Wang, "Efficient computation for sparse load shifting in demand side management," *IEEE Transactions on Smart Grid*, vol. 8, no. 1, pp. 250–261, 2017.

[29] J. Zazo, S. Zazo, and S. V. Macua, "Robust worst-case analysis of demand-side management in smart grids," *IEEE Transactions on Smart Grid*, vol. 8, no. 2, pp. 662–673, 2017.

[30] P. Li, H. Wang, and B. Zhang, "A distributed online pricing strategy for demand response programs," *IEEE Transactions on Smart Grid*, vol. 10, no. 1, pp. 350–360, Jan 2019.

[31] L. D. Collins and R. H. Middleton, "Distributed demand peak reduction with non-cooperative players and minimal communication," *IEEE Transactions on Smart Grid*, vol. 10, no. 1, pp. 153–162, Jan 2019.

[32] A. H. Mohsenian-Rad, V. W. S. Wong, J. Jatskevich, R. Schober, and A. Leon-Garcia, "Autonomous demand-side management based on game-theoretic energy consumption scheduling for the future smart grid," *IEEE Transactions on Smart Grid*, vol. 1, no. 3, pp. 320–331, Dec 2010.

[33] H. M. Soliman and A. Leon-Garcia, "Game-theoretic demand-side management with storage devices for the future smart grid," *IEEE Transactions on Smart Grid*, vol. 5, no. 3, pp. 1475–1485, May 2014.

[34] M. Latifi, A. Khalili, A. Rastegarnia, and S. Sanei, "Fully distributed demand response using the adaptive diffusion-stackelberg algorithm," *IEEE Transactions on Industrial Informatics*, vol. 13, no. 5, pp. 2291 – 2301, May 2017.
[35] L. Zhao, W. Zhang, H. Hao, and K. Kalsi, "A geometric approach to aggregate flexibility modeling of thermostatically controlled loads," *IEEE Transactions on Power Systems*, vol. 32, no. 6, pp. 4721–4731, Nov 2017.
[36] H. Hao, B. M. Sanandaji, K. Poolla, and T. L. Vincent, "Aggregate flexibility of thermostatically controlled loads," *IEEE Transactions on Power Systems*, vol. 30, no. 1, pp. 189–198, Jan 2015.
[37] F. Luo, Z. Y. Dong, K. Meng, J. Wen, H. Wang, and J. Zhao, "An operational planning framework for large-scale thermostatically controlled load dispatch," *IEEE Transactions on Industrial Informatics*, vol. 13, no. 1, pp. 217–227, Feb 2017.
[38] C. Buratti, P. Ricciardi, and M. Vergoni, "Hvac systems testing and check: A simplified model to predict thermal comfort conditions in moderate environments," *Applied Energy*, vol. 104, pp. 117 – 127, 2013.
[39] R. Deng, Z. Yang, M. Y. Chow, and J. Chen, "A survey on demand response in smart grids: Mathematical models and approaches," *IEEE Transactions on Industrial Informatics*, vol. 11, no. 3, pp. 570–582, June 2015.
[40] Z. Liu, Q. Wu, S. Huang, L. Wang, M. Shahidehpour, and Y. Xue, "Optimal day-ahead charging scheduling of electric vehicles through an aggregative game model," *IEEE Transactions on Smart Grid*, vol. PP, no. 99, pp. 1–1, 2017.
[41] J. Norstad, "An introduction to utility theory, update," http://www.norstad.org/finance/util.pdf, update: Nov. 3, 2011, Access date: Feb. 1, 2012, Mar. 29, 1999.
[42] R. Faranda, A. Pievatolo, and E. Tironi, "Load shedding: A new proposal," *IEEE Transactions on Power Systems*, vol. 22, no. 4, pp. 2086–2093, Nov 2007.
[43] P. Samadi, H. Mohsenian-Rad, R. Schober, and V. W. S. Wong, "Advanced demand side management for the future smart grid using mechanism design," *IEEE Transactions on Smart Grid*, vol. 3, no. 3, pp. 1170–1180, Sept 2012.
[44] S. Leyffer, "Integrating sqp and branch-and-bound for mixed integer nonlinear programming," *Computational optimization and applications*, vol. 18, no. 3, pp. 295–309, 2001.
[45] M. Shahidehpour and Y. Fu, "Benders decomposition in restructured power systems," *IEEE Techtorial*, no. April, 2005.
[46] C.-C. Hong and Y.-H. Huang, "A method to convert integer variables of mixed integer programming problems into continuous variables," in *Proceedings of 2013 4th International Asia Conference on Industrial Engineering and Management Innovation (IEMI2013)*, Springer, 2014, pp. 1023–1033.
[47] S. Boyd, N. Parikh, E. Chu, B. Peleato, and J. Eckstein, "Distributed optimization and statistical learning via the alternating direction method of multipliers," *Foundations and Trends® in Machine Learning*, vol. 3, no. 1, pp. 1–122, 2011.
[48] Z. J. Towfic and A. H. Sayed, "Adaptive penalty-based distributed stochastic convex optimization," *IEEE Transactions on Signal Processing*, vol. 62, no. 15, pp. 3924–3938, Aug 2014.
[49] M. S. Bazaraa, H. D. Sherali, and C. M. Shetty, *Nonlinear programming: theory and algorithms*. John Wiley & Sons, 2013.
[50] F. S. Cattivelli and A. H. Sayed, "Diffusion lms strategies for distributed estimation," *IEEE Transactions on Signal Processing*, vol. 58, no. 3, pp. 1035–1048, 2010.
[51] A. H. Sayed, *Diffusion adaptation over networks*. Academic Press Library in Signal Processing, 2013, vol. 3.
[52] ——, *Fundamentals of adaptive filtering*. John Wiley & Sons, 2003.
[53] C. G. Lopes and A. H. Sayed, "Incremental adaptive strategies over distributed networks," *IEEE Transactions on Signal Processing*, vol. 55, no. 8, pp. 4064–4077, 2007.
[54] A. H. Sayed *et al.*, "Adaptation, learning, and optimization over networks," *Foundations and Trends® in Machine Learning*, vol. 7, no. 4-5, pp. 311–801, 2014.
[55] V. D. Blondel, J. M. Hendrickx, A. Olshevsky, and J. N. Tsitsiklis, "Convergence in multiagent coordination, consensus, and flocking," in *Decision and Control, 2005 and 2005 European Control Conference. CDC-ECC'05. 44th IEEE Conference on*. IEEE, 2005, pp. 2996–3000.
[56] N. Metropolis, A. W. Rosenbluth, M. N. Rosenbluth, A. H. Teller, and E. Teller, "Equation of state calculations by fast computing machines," *The journal of chemical physics*, vol. 21, no. 6, pp. 1087–1092, 1953.
[57] F. S. Cattivelli, C. G. Lopes, and A. H. Sayed, "Diffusion recursive least-squares for distributed estimation over adaptive networks," *IEEE Transactions on Signal Processing*, vol. 56, no. 5, pp. 1865–1877, 2008.
[58] L. Xiao, S. Boyd, and S. Lall, "A scheme for robust distributed sensor fusion based on average consensus," in *Proceedings of the 4th international symposium on Information processing in sensor networks*. IEEE Press, 2005, p. 9.
[59] J. Fernandez-Bes, J. Arenas-Garcia, and A. H. Sayed, "Adjustment of combination weights over adaptive diffusion networks," in *Acoustics, Speech and Signal Processing (ICASSP), 2014 IEEE International Conference on*. IEEE, 2014, pp. 6409–6413.
[60] C.-K. Yu and A. H. Sayed, "A strategy for adjusting combination weights over adaptive networks," in *Acoustics, Speech and Signal Processing (ICASSP), 2013 IEEE International Conference on*. IEEE, 2013, pp. 4579–4583.
[61] S.-Y. Tu and A. H. Sayed, "Optimal combination rules for adaptation and learning over networks," in *Computational Advances in Multi-Sensor Adaptive Processing (CAMSAP), 2011 4th IEEE International Workshop on*. IEEE, 2011, pp. 317–320.
[62] J. Chen and A. H. Sayed, "Diffusion adaptation strategies for distributed optimization and learning over networks," *IEEE Transactions on Signal Processing*, vol. 60, no. 8, pp. 4289–4305, Aug 2012.
[63] P. Tabuada, "Event-triggered real-time scheduling of stabilizing control tasks," *IEEE Transactions on Automatic Control*, vol. 52, no. 9, pp. 1680–1685, 2007.
[64] *Pennsylvania-New Jersey-Maryland Interconnection (PJM) electricity market*, 2019. [Online]. Available: https://www.pjm.com/markets-and-operations/etools/data-miner-2/data-availability.aspx
[65] H. Mortaji, S. H. Ow, M. Moghavvemi, and H. A. F. Almurib, "Load shedding and smart-direct load control using internet of things in smart grid demand response management," *IEEE Transactions on Industry Applications*, vol. 53, no. 6, pp. 5155–5163, 2017.